PSHA input model documentation for Caribbean and Central America (CCA)

GEM Hazard Team

Version history

Table 1 summarises version history for the CCA input model, named according to the versioning system described here, and indicating which version was used in each of the global maps produced since 2018. Refer to the GEM Products Page for information on which model versions are available for various use cases. The changelog describes the changes between consecutive versions and are additive for all versions with the same model year.

Table 1 – *Version history for the CCA input model.*

Version	2018.1	2019.1	2022.1	2023.1	Changelog
v2018.0.0	X				First version of the model developed within the CCARA project.
v2019.0.0		X	X		Updated version of the model developed by GEM. The following changes were made to the source model: updated subduction model for CAM, LAN, PRC and SAM (Colombia-Ecuador segment); and new subduction sources for PAN and LMT; updated gridded seismicity, and fault sources. A new ground motion logic tree was used based on residual analysis between candidate GMPEs and strong motion recordings from the region. In general, the hazard has increased in Puerto Rico and northern Panama, and decreased in Guatemala, El Salvador, Nicaragua, and southern Panama.
v2019.1.0				X	Mmin extended to M4 for crustal distributed seismicity. gmmLT.xml updated with more recent GMPEs. The intraslab source files were consolidated into a single one per subduction zone, which revealed that some magnitudes had been missing from the former ssmLT and thus the hazard increases fractionally in places.

The following text describes v2019.1.0.

Authors: J. Garcia-Pelaez, R. Gee, R. Styron, V. Poggi

1 Summary

This model covering the Central America and the Caribbean region (CCA) was developed in the framework of the CCARA project (CCARA project) a GEM collaboration project funded by USAID. Cuba and Puerto Rico were included *a posteriori* by GEM hazard team. During the CCARA project and after it some local organizations and experts were involved and this models benefits of it: University of Costa Rica, Costa Rica - Costa Rican Institute of Electricity, Costa Rica - Nicaraguan Institute of Territorial Studies, Nicaragua - Catholic University of El Salvador, El Salvador - Ministry of Environment and Natural Resources, El Salvador - Panama University, Panama, Puerto Rico Seismic Network, Puerto Rico, National Center for Seismological Research, Cuba. The model was built as a combination of a shallow model, where active faults and distributed seismicity sources were integrated, and a subduction model, divided into its main components (i.e. interface and in-slab). The interface seismicity was modelled using complex faults, while for the in-slab region, the typology of source preferred was the non-parametric source. A publication on the model is currently in preparation.

2 Tectonic overview

The Caribbean and Central American region is broadly the Caribbean tectonic plate and vicinity (see Figure 1). The northern and southern margins of the Caribbean plate are characterized by transpressive (mostly strike-slip) faulting between the Caribbean and North and South America, respectively. Bends in the major plate-boundary faults correspond to restraining and releasing zones where deformation is locally more distributed, and in the north, restraining zones are especially important because they form many of the islands of the Greater Antilles and therefore host populations concentrated close to big faults.

To the east, oceanic crust of the undifferentiated Americas ocean plate subducts under the Caribbean plate at the Lesser Antilles Trench. The islands of the Lesser Antilles are for the most part volcanoes of this subduction system. Though the evidence for large earthquakes on this subduction zone is poor as the area is under-studied, instrumental seismicity decreases from north to south. The western margin of the Caribbean plate is a subduction zone, the Middle America Trench, where the Nazca ocean plate subducts under the Caribbean. This subduction became oblique near Panama, and a strike-flip fault zone extends along the volcanic arc from Costa Rica through Guatemala, creating localized seismic hazard in populated areas throughout Central America.

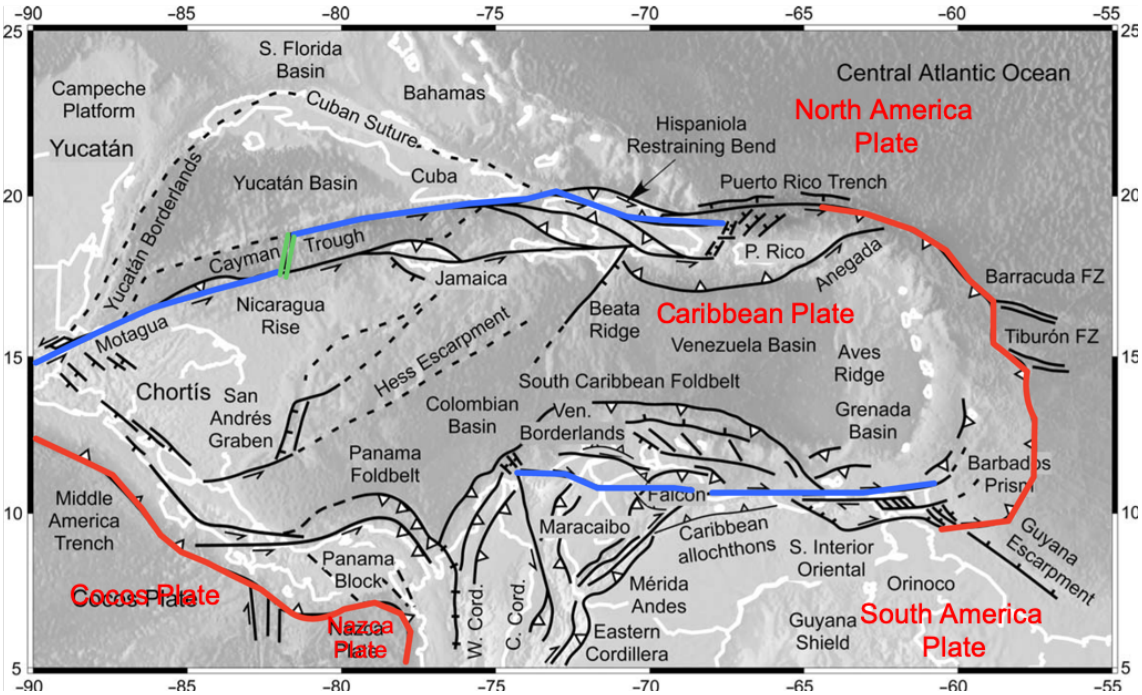

Figure 1 – *The Central America and the Caribbean Tectonics (modified from Pindell and Kennan, 2009*

3 Basic Datasets

This model was created using a compilation of basic databases needed for PSHA (i.e. parametric catalogue, focal mechanisms, active faults, strong motion recordings), which were created following common standards and transparent procedures. These databases were completed mainly by GEM, but the local expert's contribution was crucial.

3.1 Earthquake related Catalogues

A homogeneous earthquake catalogue is a fundamental requirement for any seismic hazard analysis. Here, using information from a wide collection of earthquake databases, covering in a different manner the region (see Figure 2), a parametric harmonized catalogue to be used in PSHA calculations was created for the CCA region (*Garcia and Poggi. 2017a*, see Figure 3). In addition, using information from literature, global datasets (e.g. GCMT, NEIC, ISC) and local seismic networks operating in the CCA region a dataset of focal mechanisms contained 2580 events (3429 solutions) was also compiled (see details in *Garcia and Poggi, 2017b*).

To obtain the CCA catalogue we followed an approach similar to the one used in other GEM models/projects (*Weatherill et al., 2016*; *Garcia et al., 2017*; *Poggi et al., 2017*). It contains 81538 events with $3.0 \geq M_w \geq 8.1$ from 1502 to 2016 (see Figure 3). This catalogue was

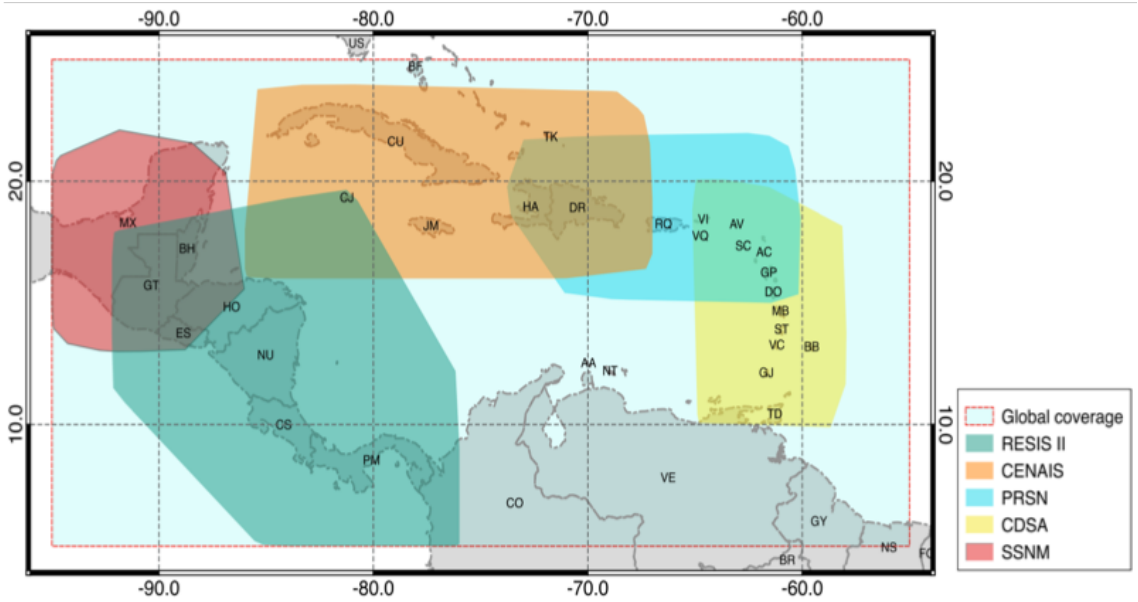

Figure 2 *– Datasets of sources used to create the CCA catalogue: Global coverage: ISC, GEM-ISC, GEM-ISC extended, GCMT; regional coverage: Resis II, CENAIS, PRSN, CDSA and SSNM.*

then purged from fore- and aftershock sequences and possible seismic swarms, using the *Gardner and Knopoff (1974)* declustering algorithm and a spatial-time *Uhrhammer (1985)* window (see details in Characterization and processing of seismic catalogues and/or the references cited above).

3.2 Fault Database

A database of *259* active faults (Figure 4) was created to study the contribution of neo-tectonic structures to seismic hazard as part of the CCARA project. The database consists in fault traces locations and related attributes describing both, geometry and kinematics (i.e. slip rates, dip angle, etc.). Details about the creation and characterization of the fault can be found in (*Styron et al., 2019*, under review for Nat. Hazards Earth Syst. Sci). The faults are publicly available on GitHub in a variety of vector formats.

3.3 Ground Motion Database

Strong motion recordings were collected for the regions of El Salvador and the Lesser Antilles. Data from the Lesser Antilles was retrieved from the Engineering Strong-motion (ESM) website, while the Ministry of the Environment (MARN) provided the recordings for El Salvador in the context of a bilateral collaboration with GEM. A total of 1239 and 600 3-component recordings were collected for El Salvador and the Lesser Antilles, respectively (Figure 5). Events were classified into different tectonic regions based on their locations. For the Lesser Antilles, classification was based on the location of the earthquakes, while

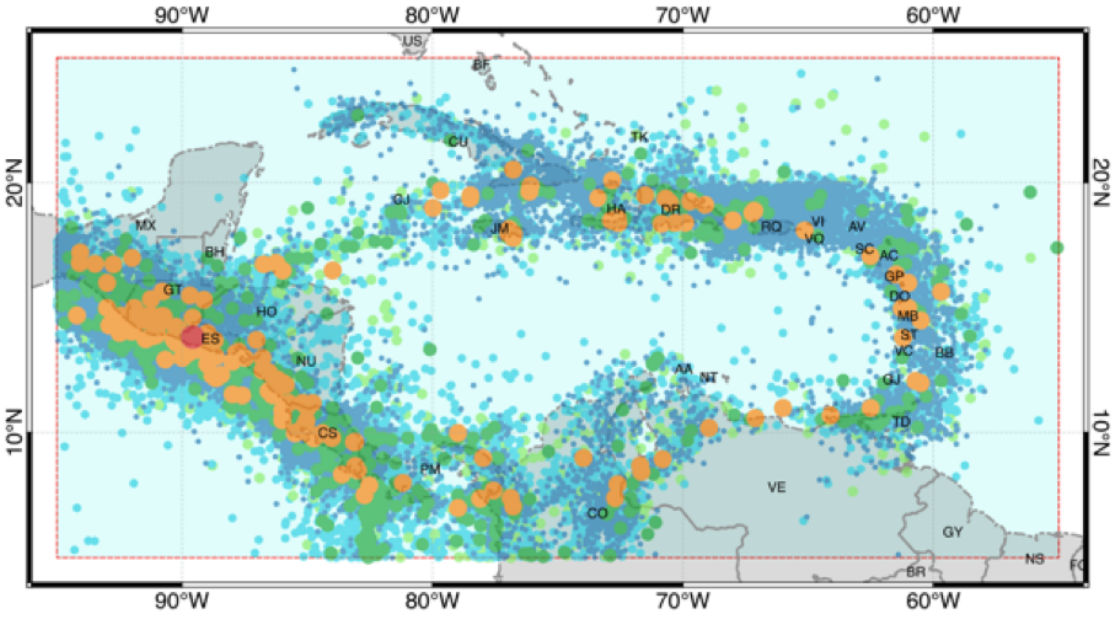

Figure 3 *– Harmonized earthquake catalogue for the CCA region.*

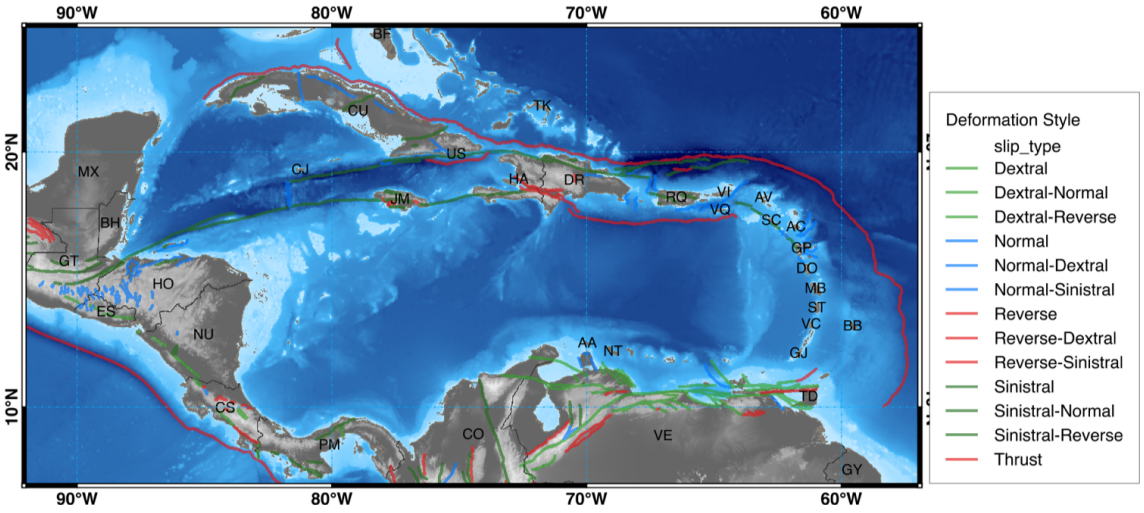

Figure 4 *– The GEM active fault database for CCA region. Different colors are used to represent the average deformation style.*

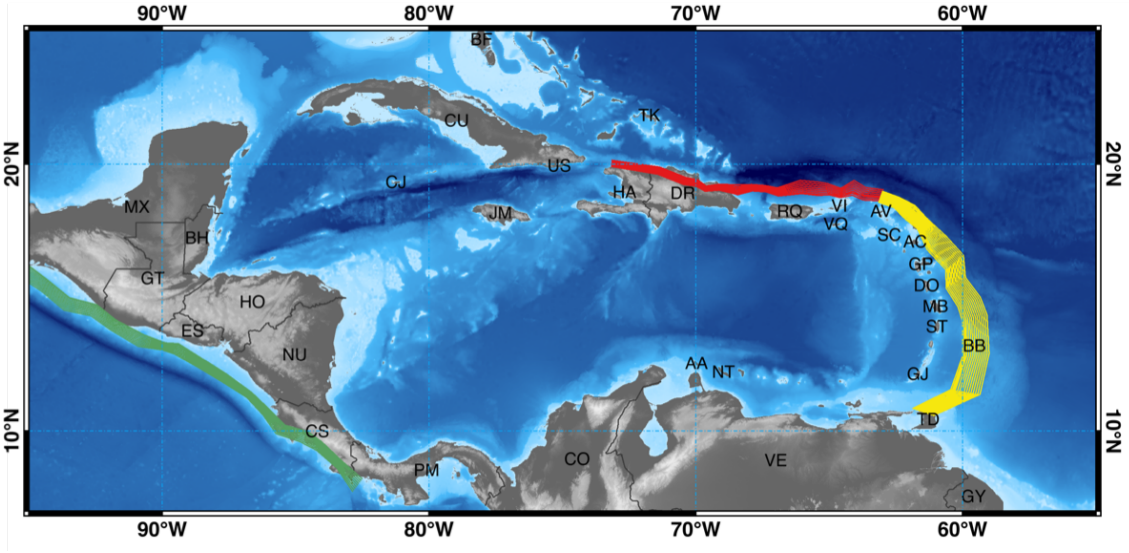

Figure 5 *– The GEM strong ground motion database for CCA region. Events were classified into tectonic region type; INT = subduction interface, SLB = subduction intraslab, ASC = active shallow crust, and UND = undefined.*

for El Salvador classification was provided in the metadata. The stations were assigned Vs30 values. For both El Salvador and the Lesser Antilles, the Vs30 values were estimated from topography since no additional information was available about site conditions.

4 Hazard Model

4.1 Seismic Source Characterisation

The Seismic Hazard Model (SHM) was built taking into account the different tectonic settings of the CCA region. It was divided into three main components:

1. The **shallow seismicity** modelled using an integrated model of **distributed seismicity** (kernel based of gridded **point sources**) and **"simple" crustal fault** sources with *Mw>6.5*;
2. The **subduction interface** seismicity modelled as large **"complex" fault** sources with a 3D geometry and *Mw>6.0*;
3. The **subduction in-slab and deep** seismicity modelled as **nonparametric ruptures** with *Mw>6* and depth < *300 km*.

Shallow seismicity: Distributed Seismicity The active shallow hazard component benefits of previous PSHA studies (*Benito et al., 2012*; *Garcia et al., 2003, 2008*; *Mueller et al.,*

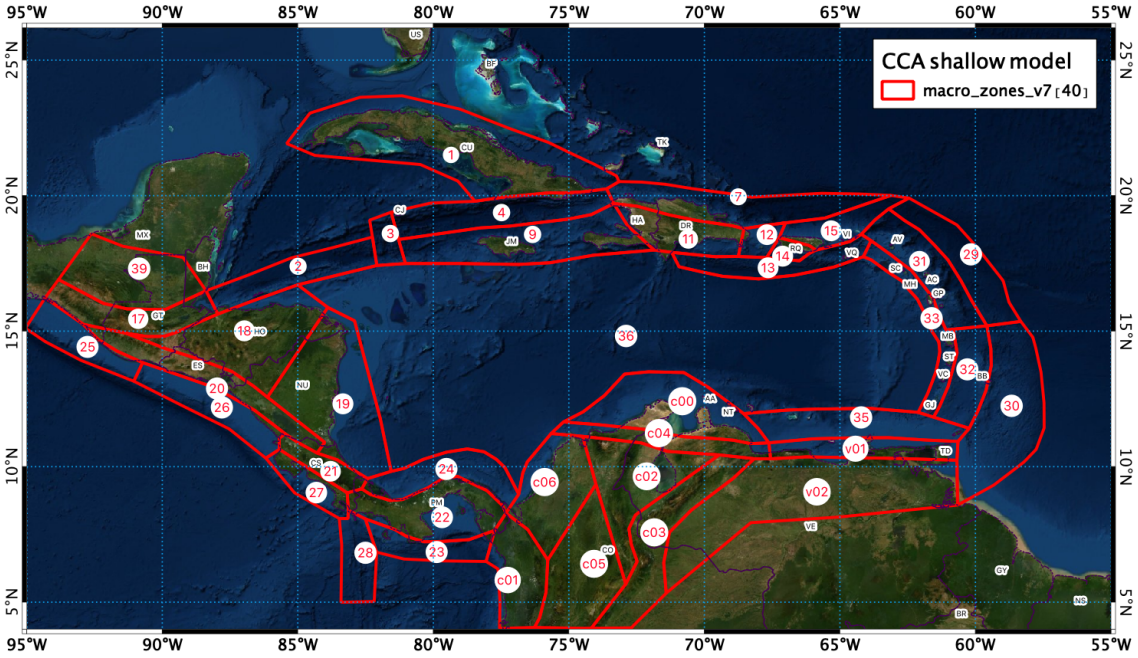

Figure 6 – *Shallow source macro-zonation for the Central America and the Caribbean region.*

2003; *Bozzoni et al., 2011*; *Salazar et al., 2014*; *Wong et al., 2019*) and GEM models covering part of the CCA region. To define the distributed seismicity model, initially, the region was discretized into *40* independent source zones (see Figure 6). These areas are represented as polygons (or volumes) delineating regions with homogeneous temporal and spatial characteristics of seismicity, tectonic and kinematic settings. Note that we are including also sources for Colombia and Venezuela.

To characterize the sources the catalogue was our main resource. A sub-catalogue produced by the regionalization procedure was used to derive the parameters characterizing the sources after that declustering and completeness analysis were performed. The parameters characterizing the sources are:

- the maximum magnitude (*Mmax*, adding an increment of *0.3* to the largest observed event),
- the seismogenic thickness (upper - *0 km* - and lower - *40 km* - seismogenic depths, constrained using hypocentres of instrumental seismicity and Moho depth definition a a regional scale),
- the focal depth distribution of events and its probability (corresponding to a histogram describing the hypocentral depth distribution from past seismicity),
- the most-likely orientation and faulting styles of ruptures (obtaining using tectonic information and the focal mechanisms distribution),
- the activity rate or magnitude frequency distribution, MFD (represented by a truncated Gutenberg-Richter distribution assuming a magnitude binning of 0.1, a mini-

mum magnitude around M_W4.5; and b and a values computed using the maximum likelihood estimator proposed by *Wiechert, (1980)*.

To model the shallow distributed seismicity, we transformed the area sources described above in a grid of point sources using a smoothed seismicity approach (Frankel, 1995). Smoothed seismicity is modelled similarly to area sources, but rather than using constant a- and b-values, the moment rates are based on observed occurrences. Essentially, we smooth the occurring seismicity onto a grid of points. The advantage of use this approach is the use of larger source zones (see Figure 8), while still capturing spatial variability in seismicity rate. The smoothed seismicity grid (spacing at 0.1°) was obtained by applying a Gaussian filter to each area source declustered sub-catalogue, and computing the fraction of spatial seismicity rates at each grid node. Then, this was combined with the MFD of the source to create a grid of point sources, each of it with its own earthquake occurrence rate. To avoid double counting of seismicity, the MFDs of point sources around fault sources were truncated at M_W6.5. A summary of main parameters of shallow/crustal sources is presented in Table 2.

SZ	***a***	***b***	$M_{max,obs}$	**Description**
01	4.97273	1.174	7.50	Cuba intraplate region
02	4.28214	0.854	7.37	Swan Islands fault zone
03	2.59765	0.626	6.10	Mid-Cayman spreading center
04	5.35133	1.094	7.50	Oriente fault system zone
07	4.64272	0.985	7.70	North Hispaniola deformed belt zone (Septentrional microplate)
09	4.36093	0.949	7.80	Gonave microplate
11	2.75507	0.637	7.50	Hispaniola microplate
12	3.27162	0.828	6.40	Mona Rift zone
13	4.37902	1.093	7.50	Los Muertos trough zone (shallow seismicity)
14	3.32206	0.925	6.57	Puerto Rico southern zone
15	3.24560	0.792	6.57	Puerto Rico northern zone
17	5.17624	1.059	7.81	Polochic-Motagua fault system zone
18	5.14075	1.045	7.20	Honduras inland extensional zone
19	4.90361	1.043	7.00	Depresion de Nicaragua zone
20	4.31061	0.799	7.90	Central America Volcanic arc zone
21	5.23234	1.088	7.65	Central Costa Rica deformed belt zone
22	4.99332	1.036	7.75	Panama microplate/block zone
23	4.73501	0.977	7.80	Southern Panama deformed belt
24	4.63410	1.023	7.90	Northern Panama deformed belt
25	4.37336	0.963	6.40	Shallow seismicity offshore Mexico-Guatemala zone
26	4.68727	0.864	7.65	Shallow seismicity offshore El Salvador-Nicaragua zone
27	4.87991	1.030	7.52	Shallow seismicity offshore Costa Rica zone
28	5.12585	0.907	7.50	Panamá Fracture zone

29	4.16454	1.003	6.17	Northern Lesser Antilles deformation front
30	3.58910	0.832	6.66	Southern Lesser Antilles deformation front
31	5.39022	1.240	7.80	Northern Lesser Antilles volcanic arc zone
32	4.64328	1.141	7.80	Southern Lesser Antilles volcanic arc zone
33	4.08358	0.996	7.50	Seismicity related to active faults system in the inner arc
35	3.29041	0.864	7.69	Northern Venezuela zone
36	4.47285	0.960	7.10	“Rigid” area of the Caribbean plate
39	4.72758	0.987	6.80	Northern Guatemala-Chiapas zone
c00	3.72478	0.860	6.35	Guajira-Paraguana northern Colombia zone (Bonaire block)
c01	4.63955	0.896	7.20	Atrato-Murindo suture zone (Choco block)
c02	3.73505	0.849	5.71	Triangular Maracaibo (block) zone
c03	4.66266	0.938	7.60	Colombian-Venezuelan Piedmont zone
c04	4.27833	1.018	6.40	Oca-Ancón fault system zone
c05	5.04691	1.092	7.01	Colombian North Andean zone
c06	4.28286	0.966	6.55	Caribbean-Colombian northeastern zone
v01	4.45622	0.930	7.31	San Sebastian-El Pilar-Costa Norte fault systems zone
v02	3.35288	0.795	6.50	Southern Venezuelan (Amazonian) zone

Table 2 *– SZ: Source Zone id. Seismicity parameters used in the CCA model. The GR a-value is related to the area source.*

Shallow seismicity: Crustal fault

Despite of largest crustal destructive events had been associated to active faults, characterization of active faults to be used as source fault into PSHA is a relatively recent development. In addition, several methodologies exist. Here, we are describing the GEM method to build an active fault model from a database of neotectonic active fault as those presented above. This database was created to be used in PSHA, then the faults were characterized (i.e. geometry and kinematic settings) following the OpenQuake standards. Some faults were updated or added recently (e.g. El Salvador, Jamaica, Cuba, on-shore Puerto Rico).

Some assumptions were used to build the model: - The occurrence of the events on the fault follows a double-truncated Gutenberg-Richter (GR) distribution, and the total seismic moment rate from the MDF equals the geological moment rate derived from the fault dimension (area) and slip rate, - The double-truncated distribution is computed using two magnitude extremes bounds (minimum and maximum), then the rates computed above an arbitary magnitude (clipping magnitude) are used, - The a-value of the GR distribution is defined using fault slip rates either measured on the field or inferred by earthquake geologists, - The b-value on the fault is assumed to be equal to those obtained for the area source enclosed the fault (of the major part of it), - The minimum magnitude (lower bound)

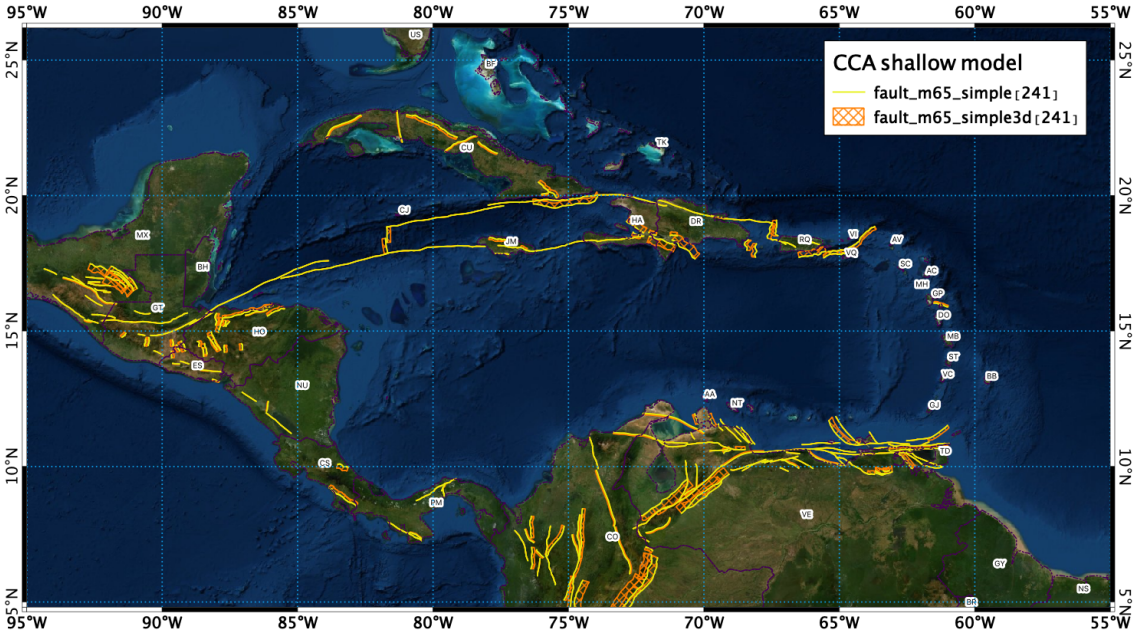

Figure 7 *– Fault sources considered for the CCA model (trace and 3d-surface projection).*

was arbitrary assumed as M_W4.0, - The maximum magnitude bounding the recurrence model depends on dimensions of the fault's area and was inferred applying *Leonard(2010, 2014)* scaling relations, - The clipping magnitude (lower bound) was arbitrary assumed as M_W6.5.

In total, we create 241 simple fault sources (see Figure 7) located in an active shallow crust tectonic regime and comprising the most hazardous structures for inland and offshore areas in the CCA region. Exceptionally, this version of the model do not included fault sources for the Lesser Antilles area where a proper characterization of the faults from a kinematic point of view was not possible this time and it should be included in future versions.

As explained before, to avoid overlapping contributions from the faults and the background gridded point sources, the activity rates of the point sources around the fault surficial projection was truncated at *M~6.5* magnitude (lower bound limit of faults MFD). Following this assumption, earthquakes with $M \geq 6.5$ can occur on the fault sources (when they are present), otherwise, the area source activity rate prevails. In Figure 8 we presenting an example of this integration for faults located in the northern part of the Hispaniola. The red dashed line (and red points) represent the seismic activity rate for the background (gridded) sources, while the yellow lines are related with contribution of each single fault. The blue line is the total (summed) contribution of the faults. For this particular case, the seismic "productivity" of gridded sources is comparable with those computed using tectonic (faults).

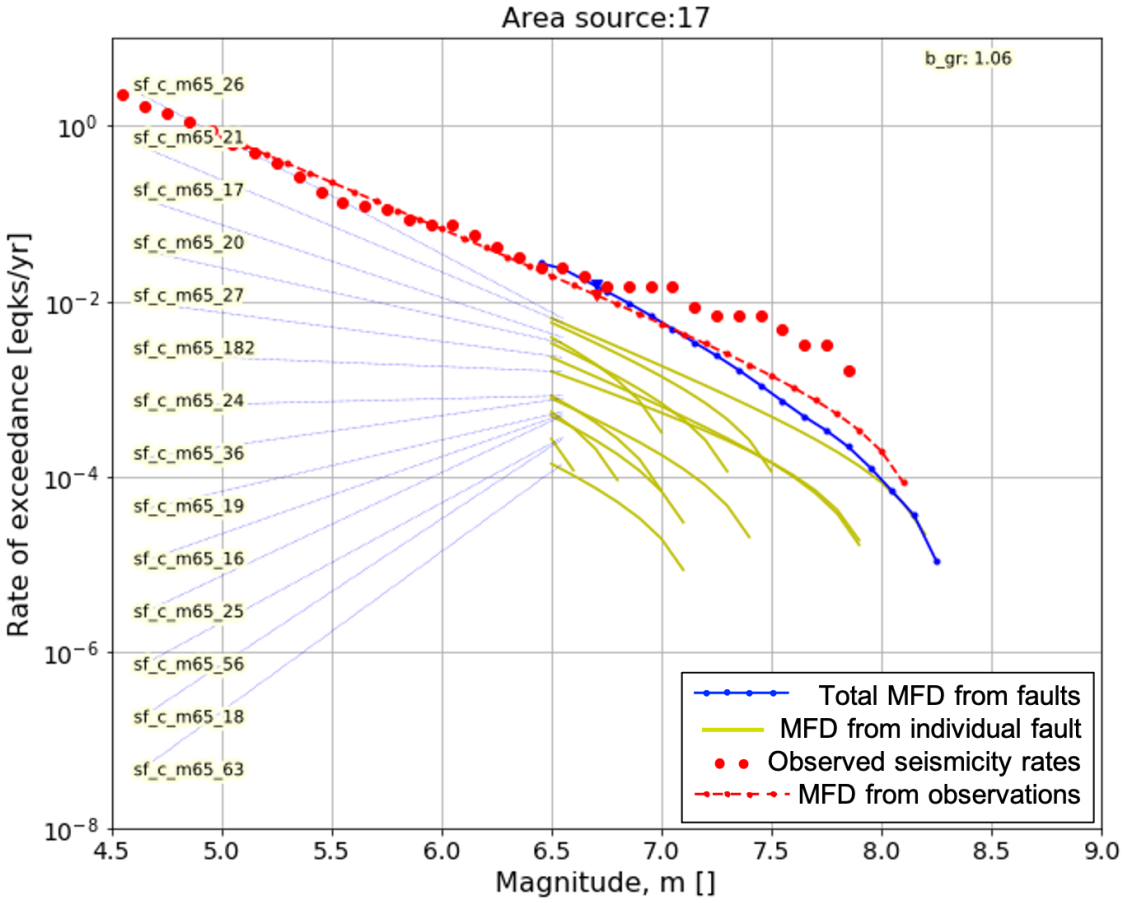

Figure 8 *– Comparison of seismic contribution of distributed seismicity and faults located inside a source zone for the Polochic-Motagua boundary plate zone. All MFDs are shown are cumulative.*

Subduction model For this version of the CCA model we are considered five subduction models with sources for Central America, Lesser Antilles and Puerto Rico - Hispaniola regions. A brief description is presented in the next lines.

The Central America model: Most of the Central America countries are located in the northwestern corner of the Caribbean Plate (CAR). The western CAR boundary is essentially a subduction zone extended along the Pacific coast from Panama to southern Mexico (*Molnar and Sykes, 1969*; *Hayes et al., 2014, 2018*) and tectonically limited by the Middle America Trench (MAT). Here the Cocos Plate (CO) subduct under CAR plate at a convergence rate of 70-90 mm/yr (*DeMets et al., 2010*; *Protti et al., 2012*). This caused active volcanism (Central America Volcanic Front, CAVF) and very high seismic activity at shallow and intermediate depth. The Southern Panama Deformed Belt (SPDB) is considered the tectonic boundary between CAR and Nazca plates, while the Polochic-Motagua fault system in Guatemala limited the CAR - North America western plate boundary. Considerable changes of slab shape (dip and orientation) along southern Costa Rica have been recognized by several authors (*Trenkamp et al., 2002*; *Vargas and Mann, 2013*), suggesting that Panama, part of Costa Rica and north-western Colombia could be part of a unique block or micro-plate, called Panama microplate . Several destructive events (M>7.5) are reported in historical catalogues and dedicated studies associated to inter -and intra- plate seismogenic sources.

The Puerto Rico - Hispaniola model: The Puerto Rico and Hispaniola (where Haiti and the Dominican Rep. are located) Islands lie close to the northeastern corner of the CAR Plate, where a slow subduction of the North America (NAM) plate beneath the CAR plate take place, dominating the tectonic environment of the region (*DeMets et al., 2000*, *Mann et al., 2002, 2005*). The angle between direction of plate motion and and the faults in its boundary help to understand the type of faulting and structural styles, with zones of transpression in southern Cuba, oblique collision between Hispaniola and the Bahama platform, oblique subduction of oceanic crust beneath Puerto Rico and north-western of Hispaniola, and orthogonal (or almost frontal) subduction at the Lesser Antilles islands arc (next subduction model). Given the complexity of tectonic settings, only recently it has been possible to know the rates and directions of interplate motion of CAR plate. *DeMets et al. (2000)* shows that CAR plate is moving at a rate of ~18 - 20 mm/yr to the east-northeast (070°). In this context the Virgin Islands and Puerto Rico are moving with CAR plate (forming the Puerto Rico - Virgin Islands micro-plate (PRVI) as proposed by Mann et al., 2005), while the Hispaniola moves independently as a detached and complex block of the CAR plate. *Jansma and Mattioli (2005)* evidenced that differential motion (~5 mm/yr) between PRVI and the Hispaniola is accommodated by slow rifting in the Mona Passage, which separate western Puerto Rico and eastern Hispaniola. The record of large earthquakes and tsunamis in this region is longest and recognized, compilations of historic information reveals that cities as Santiago de Cuba (Cuba), Port-au-Prince (Haiti), Santo Domingo (Dominican Republic), have experienced repeated damaging events in the past (*Calais et al., 1998*; *MacCann, 1985*; *Doser et al.,2005* among others). Paleoseismology studies in this region (e.g. *Prentice et al,. 2003, 2010*) reveals that recurrence of major fault ruptures could be estimated in hundreds or thousands of years.

The Lesser Antilles model: The Lesser Antilles are an active volcanic arc created by the subduction of Atlantic oceanic crust beneath the CAR plate (*Feuillet et al., 2002, 2010*). This "curved" subduction zones extending around 850 km long Lesser Antilles form the eastern margin of the CAR plate, accommodating the ENE motion (~18 - 20 mm/yr) between the NAM and the CAR plates. The seismogenic potential of this subduction has been considered as moderate (*Berryman et al., 2015*), due that associated largest earthquakes are historical (e.g. 1690 and 1843, M> 7.0) and no M8+ have been reported since 19th century. Some authors considered that it is due to the plate boundary is likely decoupled and convergence is then accommodated mostly aseismically (*Stein et al., 1982*). This assumption seems to be confirmed by recent geodetic studies (*Manaker et al., 2008*; *Symithe et al., 2015*). Nevertheless, this do not preclude the occurrence of a future large event as pointed out by *Dorel (1981)*. The instrumental seismic activity recorded by CDSA is mainly concentrated near islands arc (at 150 - 200 km of the deformation front) and associated to intense volcanism and crustal deformation. The northern sector (above 14°N) is more active than the southern one.

Nazca model: The Nazca subduction model is part of the South America Model (SAM). From SAM we used the two segments (7 and 8), describing the subduction of the Nazca plate in the pacific coast from Northern Ecuador to Southern Panama. Details about this model can be found in the documentation related with the SAM model.

North Panama Deformed Belt model: The North Panama Deformed Belt (NPDB) is the northern limit of the Panamá microplate. NPDB extends offshore the Caribbean coast of Panamá from the north-western border of Panamá and Colombia to Puerto Limón in Costa Rica. Its origin is related with the convergence between the Caribbean plate and the Panamá microplate. On this overthrust fault reverse faulting predominant and on-shore and off-shore deformation with a SW-dipping is confirmed by instrumental seismicity recorded by regional and local networks (*Camacho et al. 2010*) as well as historical large events (e.g. 1882 Panama Mw7.9 event, *Camacho and Víquez, 1993*). *Alvarado et al. (2016)* suggest a variation of tectonic regime from Panama (shallow subduction) to Costa Rica (typical thrust fault system).

"Los Muertos" Trough model: The Muertos trough a ~650 km-long deformed belt bound the Puerto Rico microplate at south of the Dominican Republic (DR) and Puerto Rico (*Mann et al. 2005*). It is considered as a active subduction zone (*Dolan et al. 1998*; *LaForge and McCann, 2005*; *McCann, 2007*) accomodating the closure between the Caribbean plate and the Puerto Rico microplate. However, *Granja Bruña et al., 2010* interpreted this zone as a retroarc thrusting using gravity modeling. The westermost limit of this deformed belt is close to the Beata fault in DR and dieng out gradually to the east transferring the plate motion to faults in the Anegada trough. The distribution of seismicity is difuse and have a high degree of uncertainty. This make the definition of the plate geometry a challenge (*Granja Bruña et al., 2010*). However, the Muertos Trough plays an important role in the tectonic of the north-eastern Caribbean plate boundary and a source zone has been created for this version of the CCA model.

The methodology utilized follows a new approach developed within the CCARA project and currently tested (and improved) in a number of different subduction areas across the world (*Pagani et al., in preparation*). The approach is divided in two main steps: the first one aiming at defining the geometry (e.g.∼top and bottom of the slab, average thickness of slab) and the structure of subduction including its possible segmentation, the second one is focused on seismic activity rate characterization of subduction sources. The starting point for the definition of the subduction geometry is the creation of a number of manually digitized profiles describing the contact between the subducted slab and the overrinding plate to define a 3D meshed surface. The profiles were obtained using cross sections along trench axis. The data plotted on the cross sections (see example in Figure 9) is meant to illuminate the subsurface subduction structures and tectonic processes that contribute to seismic hazard. The data used was:

- Best located hypocentres (CCA catalogue),
- Centroid moment tensors (CMTs) from the Global CMT project (*Dziewonski et al., 1981*; *Ekstrom et al., 2012*),
- Moho depth estimates from Lithos1.0 (*Pasyanos et al., 2014*) and Crust1.0 (*Laske et al., 2013*) models,
- Slab depth estimates from Slab2.0 (*Hayes et al., 2018*)
- Shuttle Radar Topography Mission (SRTM) topography (*Farr, 2007*)
- General Bathymetric Charts of the Ocean (GEBCO) bathymetry (*Weatherall et al., 2015*)

We model the geometry of subduction interface sources as Openquake *complex faults* and float possible ruptures (ranging specified magnitude limits from the MDF and with a given rupture aspect ratio) across the meshed surface obtained. To determinate the limits of the interface sources (i.e. portion of the contact between the slab and the overlying plate, usually considered locked) we cut the 3D mesh at two depths: *10/15* km and *40/50* km. For in-slab seismicity we used non-parametric ruptures sources. Our algorithm models ruptures at grid of points throughout the meshed approximation of the slab volume, and keeps ruptures that fit within the slab. The geometry of the ruptures with normal slip and dipping *45°* and *135°* is defined within a volume constrained at the top (below interface lower depth definition) and at the bottom by a surface obtained by projecting the in-slab-top surface 60 km toward a perpendicular direction (see Figure 10).

For the characterization of earthquake occurrence, we used a regionalized sub-catalogue generated for a specific tectonic region (e.g. Central America interface). We performed the declustering (using *Uhrhammer, 1986* windowing) and completeness analysis and estimate the occurrence rates following a double truncated Gutenberg-Richter MDF as for the shallow distributed seismicity model. The lower bound of interface MDFs is arbitrary fixed at M_w6.0 for all interface sources and at M_w6.5 for the in-slab ones. The upper bound of the MFD for interface sources was defined combining information on past seismicity and constraints from the subduction geometry and a magnitude-scaling relationship (*Strasser et al., 2009*), while for the in-slab sources the rates were distributed among the computed non-parametric ruptures.

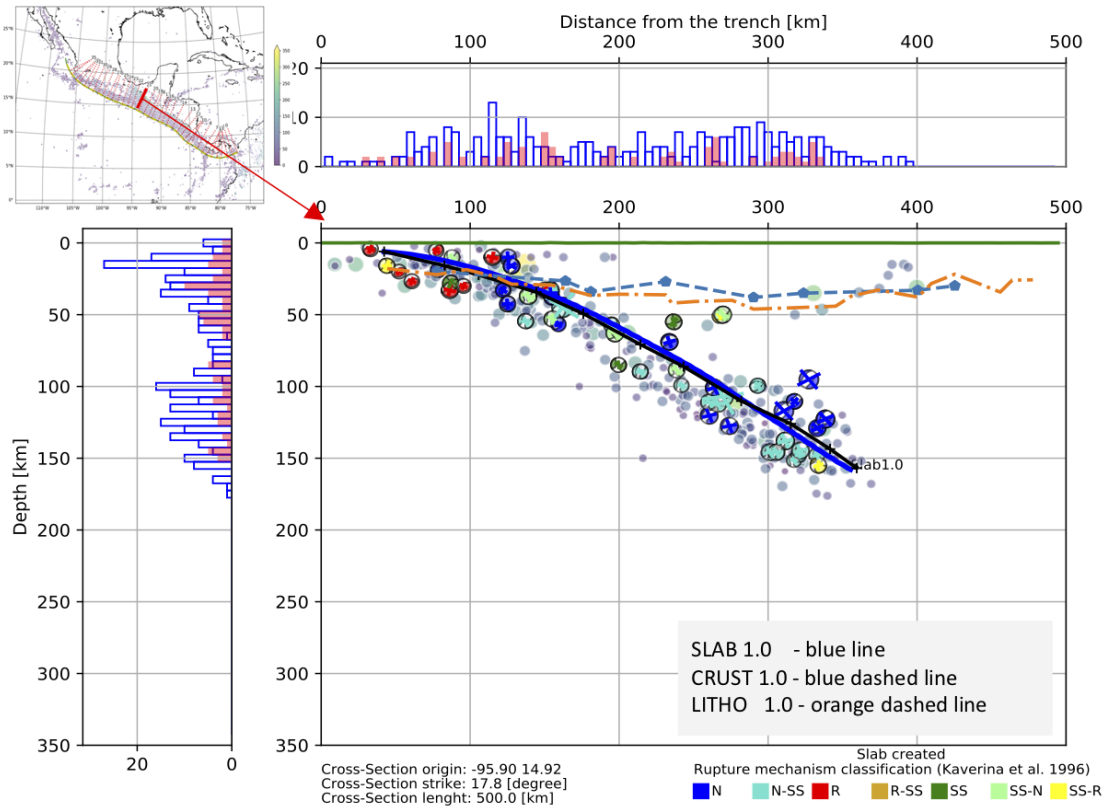

Figure 9 *– Example of cross-section describing the contact between the subducted slab and the overrinding plate. Top left shows the position of the cross section. Histograms are showing the distribution of hypocenters at each depth (bottom left) and along the profile (top right), comparing global CMT centroids (red) with catalogue hypocenters (blue).*

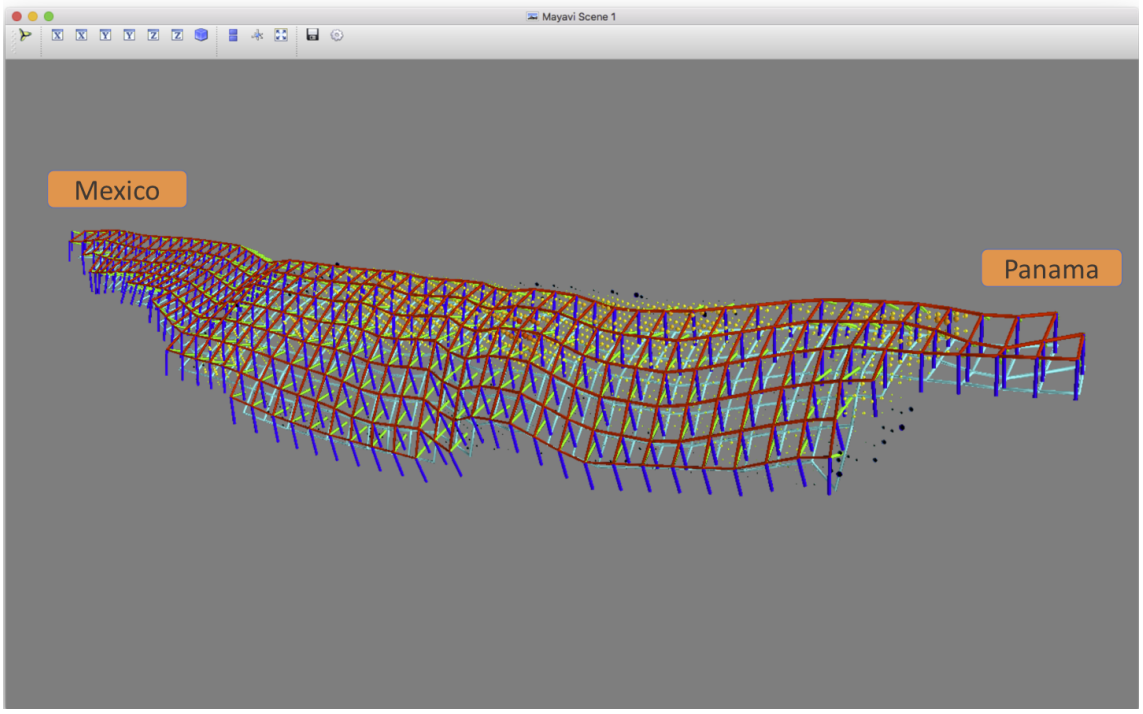

Figure 10 *– Example of 3D volume representing the portion of the subduction generating in-slab sesimicity for Central America - Mexico subduction.*

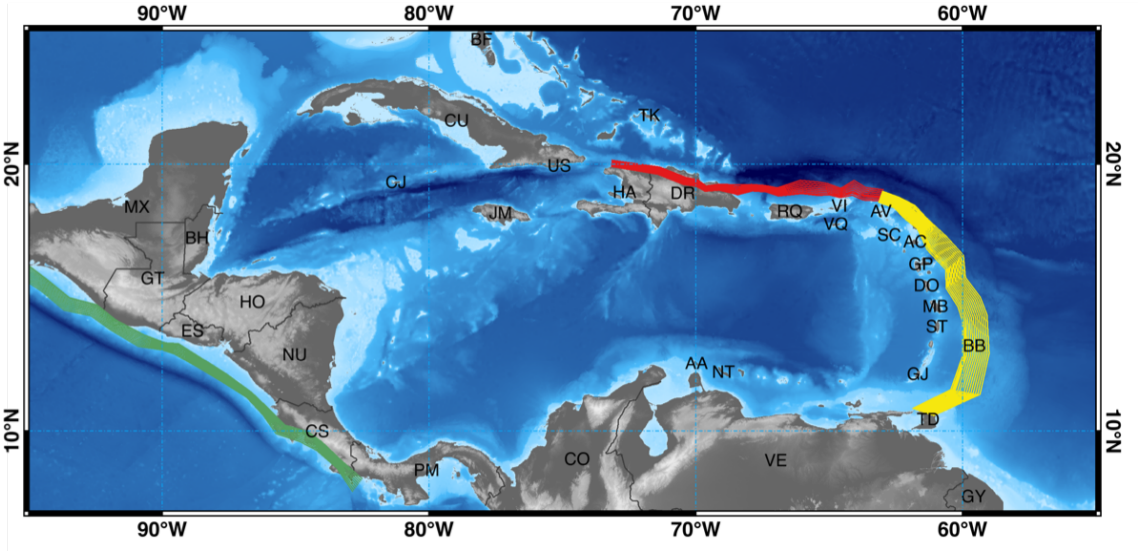

Figure 11 *– Complex faults (surface projection) characterizing the interface seismicity for the CCA region/model. CAM: the Central America model, PAN: the North Panama Deformed Belt model, LAN: the Lesser Antilles model, PRC: the Puerto Rico - Hispaniola model and LMT: "Los Muertos" Trough model.*

The GEM Subduction Toolkit was used to build all models. The geometry of the sources is presented in Figure 11 (surface projection of complex faults characterizing interface seismicity) and Figure 12 (top of surface enveloping the non-parametric sources).

In Table 3 we summarize the parameters characterizing the sources.

4.2 Ground Motion Characterization

The GMPE selection process for CCA involved three main steps. First, we pre-selected a set of about 10 candidate GMPEs from the literature for each tectonic region considered in the SSM. The pre-selection was performed using a subset of the well-established exclusion criteria proposed by *Cotton et al (2006)* and *Bommer et al. (2010)*. This was followed by a comparison of the ground motion scaling of the pre-selected GMPEs using a suite of rupture scenarios consistent with the ruptures modelled in the seismic source model. Such comparisons (referred to as trellis plots) allowed for identifying and excluding GMPEs that behave unfavourably, for example during extrapolation outside the suggested applicability range. The final step of the selection process involved comparison between the ground motions computed by the pre-selected GMPEs and the ground motions observed in the region. Data-to-model comparisons were performed by analysing the ground motion residuals (e.g. *Scherbaum et al., 2004*; *Stafford et al., 2008*) using the OpenQuake strong motion toolkit (*Weatherill, 2014*).

For the final selection we tried to achieve balance by selecting models that both over and

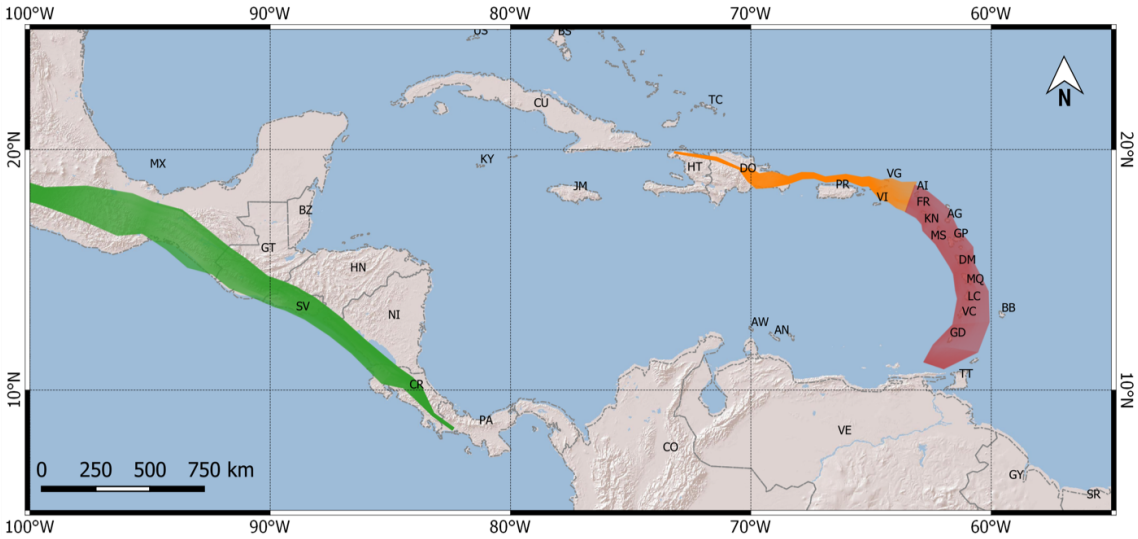

Figure 12 *– Top of surface enveloping the in-slab non-parametric sources included in the CCA model. CAM: Central America model, LAN: the Lesser Antilles model and PRC: the Puerto Rico - Hispaniola model.*

underpredict the observed ground motions in each of the tectonic regions when possible, according to the results of the residual analysis. Two notable results of the residual analysis were the observation of lower ground motions for crustal events than expected in both the Lesser Antilles and El Salvador, and differences in attenuation for intraslab earthquakes in the Lesser Antilles and El Salvador. The final GMPE logic tree is shown in Table **??**. The GMPEs selected for active shallow crust and subduction interface are the same for the Lesser Antilles and El Salvador, while for subduction intraslab they are different. Hence the logic tree distinguishes between four main tectonic regions: *Active Shallow Crust*, *Subduction Interface*, *Subduction IntraSlab* (referred to Panama - Mexico subduction), and *Subduction IntraSlab LAN_PRC*, while sources in Colombia Subduction Interface COL Subduction IntraSlab COL use the GMPEs selected with the SARA project.

Subduction Interface COL	**Weight**
AbrahamsonEtAl2015SInterHigh	0.5
MontalvaEtAl2017SInter	0.5
Subduction IntraSlab LAN_PRC	**Weight**
AbrahamsonEtAl2015SSlab	0.33
AtkinsonBoore2003SSlab	0.33
Kanno2006Deep	0.34
Subduction IntraSlab	**Weight**
Kanno2006Deep	0.33
AbrahamsonEtAl2015SSlab	0.33
ZhaoEtAl2006SSlab	0.34
SCR Non Craton	**Weight**

AkkarEtAlRjb2014	0.33
CauzziEtAl2014	0.33
AbrahamsonEtAl2014	0.34
Subduction IntraSlab COL	**Weight**
AbrahamsonEtAl2015SSlab	0.5
MontalvaEtAl2017SSlab	0.5
Subduction IntraSlab CAM	**Weight**
ZhaoEtAl2006SSlab	0.33
AbrahamsonEtAl2015SSlab	0.34
Kanno2006Deep	0.33
Subduction Interface	**Weight**
AbrahamsonEtAl2015SInter	0.33
ZhaoEtAl2006SInter	0.33
ParkerEtAl2020SInter	0.34
Active Shallow Crust	**Weight**
AkkarEtAlRjb2014	0.33
CauzziEtAl2014	0.33
AbrahamsonEtAl2014	0.34
Stable Shallow Gridded	**Weight**
NGAEastUSGSSeedB_bca10d	0.02209
NGAEastUSGSSeedB_ab95	0.00736
NGAEastUSGSSeedB_bs11	0.00736
NGAEastUSGSSeed2CCSP	0.01841
NGAEastUSGSSeed2CVSP	0.01841
NGAEastUSGSSeedGraizer16	0.01813
NGAEastUSGSSeedGraizer17	0.01813
NGAEastUSGSSeedPZCT15_M1SS	0.01813
NGAEastUSGSSeedPZCT15_M2ES	0.01813
NGAEastUSGSSeedSP15	0.03626
NGAEastUSGSSeedYA15	0.03736
NGAEastUSGSSeedHA15	0.03736
NGAEastUSGSSeedFrankel	0.03737
NGAEastUSGSSeedPEER_GP	0.0385
NGAEastUSGSSammons1	0.0492
NGAEastUSGSSammons2	0.0663
NGAEastUSGSSammons3	0.0595
NGAEastUSGSSammons4	0.0461
NGAEastUSGSSammons5	0.0304
NGAEastUSGSSammons6	0.0731
NGAEastUSGSSammons7	0.0681
NGAEastUSGSSammons8	0.0584
NGAEastUSGSSammons9	0.0573
NGAEastUSGSSammons10	0.0187

NGAEastUSGSSammons11	0.0143
NGAEastUSGSSammons12	0.0195
NGAEastUSGSSammons13	0.0117
NGAEastUSGSSammons14	0.0244
NGAEastUSGSSammons15	0.0245
NGAEastUSGSSammons16	0.0219
NGAEastUSGSSammons17	0.0236

Table 4 *– GMPEs used in the CCA model.*

Epistemic Uncertainties For this version of the model, only the epistemic uncertainty related with Ground Motion Characterization was considered (combination of three GMPEs for each tectonic environment). The model consists in a source model and 27 end-branches. In future versions, epistemic uncertainty related to Seismic Source Characterization (i.e. alternative fault model, segmented subduction model) will be considered too.

Source ID	*a*-Value	*b*-Value	M_{max}	Description
int_cam	6.78781	1.084372	8.50	Interface source for the Central America subduction model
int_lan	4.706386	0.919454	8.50	Interface source for the Lesser Antilles subduction model
int_prc	5.347351	1.041906	8.50	Interface source for the Puerto Rico-Hispaniola subduction model
int_lmt	3.158115	0.720279	7.75	Seismicity related with “Los Muertos” fault system
int_pan	3.7579408	0.818074	8.25	Seismicity related with North Panamá Deformed Belt
slab_cam	6.123138	1.014256	8.50	In-slab seismicity characterization of the Central America subduction model
slab_lan	4.509280	0.863988	8.50	In-slab seismicity characterization of the Lesser Antilles subduction model
slab_prc	4.228295	0.864203	8.00	In-slab seismicity characterization of the Puerto Rico-Hispaniola subduction model

Table 3 – *Seismicity parameters used in the CCA subduction models.*

5 Results

Hazard curves were computed with the OQ engine for the following:

- Intensity measure types (IMTs): peak ground acceleration (PGA) and spectral acceleration (SA) at 0.2s, 0.3s, 0.6s, 1.0s, and 2s
- reference site conditions with shear wave velocity in the upper 30 meters (Vs30) of 760-800 m/s, as well as for Vs30 derived from a topography proxy (Allen and Wald, 2009)

Hazard maps were generated for each reference site condition-IMT pair for 10% and 2% probabilities of exceedance (POEs) in 50 yrs. Additionally, disaggregation by magnitude, distance, and epsilon was computed for the following cities: LIST OF CITIES. The results were produced as csv files and bar plots for each of the following combinations:

- hazard levels for 10% and 2% POE in 50 yrs
- PGA and SA at 0.2s, 0.3s, 0.6s, and 1.0s
- Vs30=800 m/s

All calculations used a ground motion sigma truncation of 5. Results were computed for sites with 6 km spacing

Visit the GEM Interactive Viewer to explore the Global Seismic Hazard Map values (PGA for Vs30=800 m/s, 10% poe in 50 years). For a comprehensive set of hazard and risk results, see the GEM Products Page.

6 References

Allen, T. I., and Wald, D. J., 2009, On the use of high-resolution topographic data as a proxy for seismic site conditions Vs**30**, Bulletin of the Seismological Society of America, 99, no. 2A, 935-943

Alvarado, G.E. (2016). El cinturón deformado del norte de Costa Rica-Colombia: ¿Desde una faja de empuje-plegamiento hasta una zona de subducción incipiente dentro de un bloque o microplaca? IASPEI Regional Assembly Latin-American and Caribbean Seismological Commission - LACSC, June 20–22, San José. 39.

Bakun, W. H., C. H. Flores, and S. Uri (2012). Significant earthquakes on the Enriquillo fault system, Hispaniola, 1500–2010: Implications for seismic hazard, Bull. Seismol. Soc. Am., 102(1), 18–30.

Benito, B., Lindholm, C., Camacho, E., Climent, A., Marroquin, G., Molina, E., Rojas, W., Escobar, J.J., Talavera, E., Alvarado, G. and Torres, Y. (2012). A new evaluation of Seismic Hazard for the Central America Region, Bull. Seism. Soc. Am., 102, 2:504-523.

Bozzoni, F., Corigliano, M., Lai, C.G., Salazar, W., Scandella, L., Zuccolo, E., Latchman, J., Lynch. L., Robertson, R. (2011). Probabilistic Seismic Hazard Assessment at the Eastern Caribbean Islands. Bulletin of Seismological Society of America, 101, 5, 2499-2521.

Calais, E., Bethoux, N., and Mercier de Lepinay, B. (1992). From transcurrent faulting to frontal subduction: A seismotectonic study of the Northern Caribbean Plate boundary from Cuba to Puerto Rico, Tectonics 11, 114–123.

Camacho, E., Hutton, W., Pacheco, J.F. (2010). A new look at evidence for a Wadati–Benioff zone and active convergence at the north Panama deformed belt. Bull. Seismol. Soc. Am. 100 (1), 343–348.

Camacho, E., Víquez, V. (1993). Historical seismicity of the North Panama Deformed Belt. Rev. Geol. Am. Central 15, 49–64.

Dolan J. F. and P. Mann, editors, (1998). Active Strike-slip and Collisional Tectonics of the Northern Caribbean Plate Boundary Zone, Geological Society of America Special Paper 324, p. v-xvi.

Doser, D.I., Rodriguez, C.M., Flores, C. (2005). Historical earthquakes of the Puerto Rico-Virgin Islands region (1915-1963). In: Geol. Soc. Am., Special Paper 385. 103–114.

Doser, D. I., and Vandusen, S. R. (1996). Source processes of large (M≥6.5) earthquakes of the southeastern Caribbean (1926– 1960). Pure and Applied Geophysics, 146(1), 43-66.

Dorel, J. (1981). Seismicity and seismic gap in the lesser antilles arc and earthquake hazard in Guadeloupe, Geophys. J. Int., 67(3), 679–695.

Feuillet, N., I. Manighetti, P. Tapponnier, and E. Jacques (2002). Arc parallel extension and localization of volcanic complexes in Guadeloupe, Lesser Antilles, J. Geophys. Res., 107(B12), 2331, doi:10.1029/2001JB000308.

Feuillet, N., et al. (2010). Active faulting induced by slip partitioning in Montserrat and link with volcanic activity: New insights from the 2009 GWADASEIS marine cruise data, Geophys. Res. Lett., 37, L00E15, doi:10.1029/2010GL042556.

Garcia, J. and V. Poggi (2017a). A harmonized Earthquake Catalogue for Central America and the Caribbean region. CCARA Project. GEM Technical Report, Pavia, July 2017,

Garcia, J. and V. Poggi (2017b). A database of focal mechanisms for Central America and the Caribbean region. CCARA Project. GEM Technical Report, Pavia, July 2017,

Garcia, J., G. Weatherill, M. Pagani, L. Rodriguez, V. Poggi and the SARA Hazard Working Group (2017). "Building an open seismic hazard model for South America: the SARA-PSHA model". In Proceedings of the 16th World Conference on Earthquake Engineering, Santiago, Chile, January 2017, paper n. 2154.

Garcia J., Slejko D., Alvarez L., Peruzza L., Rebez A. (2003). Seismic hazard maps for Cuba and sorrounding areas. Bull. Seism. Soc. Am., 93, 6, pp. 2563-2590.

Garcia J., Slejko D., Alvarez L., Rebez A., Santulin M. (2008). Seismic hazard map for the Cuba region using the spatially smoothed seismicity approach, Journal of Earthquake Engineering, Vol. 12, Issue 2, pp. 173 – 196, DOI: 10.1080/13632460701512902.

Granja Bruña, J.L., Muñoz-Martín, A., ten Brink, U.S. et al. (2010). Gravity modeling of the Muertos Trough and tectonic implications (north-eastern Caribbean), Mar Geophys Res (2010) 31: 263. https://doi.org/10.1007/s11001-010-9107-8

Jansma, P.E., and Mattioli, G.S. (2005). GPS results from Puerto Rico and the Virgin Islands: Constraints on tectonic setting and rates of active faulting, in Mann, P., ed., Active Tectonics and Seismic Hazards of Puerto Rico, the Virgin Islands, and Offshore Areas: Geological Society of America Special Paper 385, p. 13–30.

Kellogg, J.N., Vega, V. (1995). Tectonic development of Panama, Costa Rica and the Colombian Andes: constraints from global positioning geodetic systems and gravity. In: Mann, P. (Ed.), Geologic and Tectonic Development of the Caribbean Plate Boundary in Southern Central America, pp. 75–90 (GSA Special Paper, 295).

Kopp, H., et al. (2011). Deep structure of the central Lesser Antilles island arc: Relevance for the formation of continental crust, Earth Planet. Sci. Lett., 304(1–2), 121–134.

Manaker, D. M., E. Calais, A. M. Freed, S. T. Ali, P. Przybylski, G. S. Mattioli, P. Jansma, C. Prépetit, and J. B. De Chabalier (2008). Interseismic plate coupling and strain partitioning in the northeastern Caribbean, Geophys. J. Int., 174(3), 889–903.

Mann, P., Calais, E., Ruegg, J.C., DeMets, C., Jansma, P. & Mattioli, G.S. (2002). Oblique collision in the northeastern Caribbean from GPS measurements and geological observations, Tectonics, 37, doi:0.1029/2001TC001304.

Mann, P., Hippolyte, J.-C., Grindlay, N.R. (2005). Neotectonics of southern Puerto Rico and its offshore margin. In: Geol. Soc. Am., Special Paper 385. 173–214.

McCann, W. R.(2007). The Muertos Trough as a major earthqauke and tsunami hazard for Puerto Rico, Eoc Trans AGU 88(23): Jt Assembly Suppl Abs S52A-03.

McCann, W. R.(1985). On the earthquake hazards of Puerto Rico and the Virgin Islands, Bull. Seismol. Soc. Am., 75, 251–262, 1985.

Mueller, C., Frankel, A., Petersen, M., and Leyendecker, E. (2010). New seismic hazard maps for Puerto Rico and the U.S. Virgin Islands, Earthquake Spectra 26, 169–186.

Molnar, P., Sykes, L.R. (1969). Tectonics of the Caribbean and Middle America regions from focal Mechanisms and seismicity. Geol. Soc. Amer. Bull. 80, 1639–1684.

Pindell J.L. and Kennan L. (2009). Tectonic evolution of the Gulf of Mexico, Caribbean and northern South America in the mantle reference frame: an update, Geological Society, London, Special Publications 2009; v. 328; p. 1-55 doi: 10.1144/SP328.1

Prentice, C.S., Mann, P., Pea, L.R. y Burr, G., (2003). Slip rate and earthquake recurrence along the central Septentrional fault, North American-Caribbean plate boundary, Dominican Republic. Journal of Geophysical Research, 108, doi:10.129/ 2001JB000442.

Prentice, C. S., P. Mann, A. J. Crone, R. D. Gold, K. W. Hudnut, R. W. Briggs, R. D. Koehler and P. Jean, (2010). Seismic hazard of the Enriquillo–Plantain Garden fault in Haiti inferred from palaeoseismology, Nature Geosciences, 3, 789-793.

Protti, M., González, V., Freymueller, J., Doelger, S. (2012). Isla del Coco, on Cocos Plate, converges with Isla de San Andrés, on the Caribbean Plate, at 78mm/year. Rev. Biol. Trop. 60 (Supl. 3), 33–41.

Salazar, W., L. Brown and G. Mannette (2013). Probabilistic Seismic Hazard Assessment for Jamaica. Journal of Civil Engineering and Architecture, ISSN 1934-7359, USA, Sep., Volume 7, No. 9 (Serial No. 70), pp. 1118-1140.

Styron, R. and García-Pelaez, J. and Pagani, M.(2020). CCAF-DB: The Caribbean and Central American Active Fault Database, Nat. Hazards Earth Syst. Sci. Discuss., 1-42, https://doi.org/10.5194/nhess-2019-46.

Symithe, S., Calais, E., de Chabalier, J.-B., Robertson, R., Higgins, M. (2015). Current block motions and strain accumulation on active faults in the Caribbean. J. Geophys. Res. 120, 1–27.

Trenkamp, R., Kellogg, J.N., Freymeuller, J.T., Mora, H.P. (2002). Wide plate margin deformation, southern Central America and northwestern South America, CASA GPS observations. J. S. Am. Earth Sci. 15, 157–171.

Vargas, C.A., Mann, P. (2013). Tearing and breaking off of subducted slabs as the result of collision of the Panama arc-indenter with northwestern South America. Bull. Seismol. Soc. Am. 103 (3), 2025–2046.

Van Dusen, S. R., and Doser, D. I. (2000). Faulting processes of historic (1917–1962) M≥6.0 earthquakes along the north-central Caribbean margin. Pure and Applied Geophysics, 157(5), 719-736.

Wong I., P. Thomas, R. Koehler, and N. Lewandowski (2019). Assessing the Seismic Hazards in Jamaica Incorporating Geodetic and Quaternary Fault Data. Bulletin of the Seismological Society of America, Vol. 109, No. 2, pp.716, 731, doi: 10.1785/0120180205

7 Methods

The PSHA input model descried herein was among the models constructed by the GEM Secretariat, and in a systematic way that uses GEM's model-building tools. These tools helped to facilitate model construction, allowing the hazard modeler to apply commonly used methods when developing seismic hazard models. The next subsections describe some of the fundamental concepts and methods used to construct this hazard model.

7.1 Distributed Seismicity Sources

We use the term "distributed seismicity" to indicate earthquakes not clearly attributable to an individual fault source or subduction zone. To model these, we group together seismicity with common characteristics, such as focal mechanism type, strain by the same tectonic forces, rate, or 3D distribution; we then produce source models reflecting these characteristics. Here, we describe two primary source types used to model distributed seismicity.

7.2 Area Sources

Area sources consist of a statistically-determined MFD (Section 11.1) from earthquakes occuring in a volume (usually a polygon, defined by the modeler, with depth limits), with the modelled occurrence rates distributed uniformly (equal *a*- and *b*-values) over an evenly spaced grid, and paired with a hypocenter and focal mechanism. In the OpenQuake Engine, the specified hypocentral depths and focal mechanisms can be probability distributions, or singular metrics.

7.3 Smoothed Seismicity

Smoothed seismicity is modeled similarly to area sources, but rather than using a spatially-homogeneous MFD in each source, the *a*-values vary spatially based on observed seismicity.

GEM has moved away from using traditional area sources, and predominantly models distributed seismicity with an approach that combines area sources with smoothed sesimicity, incorporating methods from Frankel (1995). We define a few source zones with internally consistent tectonics (e.g., up to a few prominent focal mechanism types, reflecting the same tectonic stresses), solve for the Gutenberg-Richter *b*-value, and then smooth the occurring seismicity onto a grid of points. This approach allows us to use larger source zones (and thus more earthquakes to compute a more robust MFDs) while still capturing spatial variability in seismicity rate.

We use the declustered crustal sub-catalogue, applying the *Stepp (1971)* completeness analysis or one based on time-magnitude density plots. Then, from the earthquakes within each source zone, we compute a double truncated Gutenberg-Richter MFD from M=5 to $M_{max,obs}$ + 0.5 (bins of M 0.1), solving for *a*- and *b*-values based on *Weichert (1980)*. We

classify the earthquake probability into weighted depth bins. Lastly, we assign most-likely nodal planes based on crustal earthquake focal mechanisms within the source zone based on the GCMT catalogue.

We compute the smoothed seismicity grid by applying a Gaussian filter to the clipped, declustered catalogue for each source zone, and computing the fraction of spatial seismicity rates at each grid node. These are combined with the zone MFD to compute a grid of point-by-point earthquake occurrence rates.

In areas where we also model fault sources, we prevent double counting by dividing the magnitude occurrence bins between the two source types. If there is overlap (including a buffer around the surface projection of a fault, we cut the MFDs for distributed seismicity at *Mmax*=6.5, and use the same value as *Mmin* for fault MFDs (described in Section 7.5).

7.4 References

Frankel, A. (1995). Mapping seismic hazard in the central and eastern United States. Seismological Research Letters, 66(4), 8-21.

Stepp, J. C. (1971). "An investigation of earthquake risk in the Puget Sound area by the use of the type I distribution of largest extreme". PhD thesis. Pennsylvania State University (cited on pages 9, 25–27).

Weichert, Dieter H. "Estimation of the earthquake recurrence parameters for unequal observation periods for different magnitudes." Bulletin of the Seismological Society of America70.4 (1980): 1337-1346.

7.5 Characterizing and modelling fault sources

Discrete geologic faults produce the largest earthquakes in the shallow crust. Here we describe the important characteristics of faults, and how we build fault sources for OpenQuake.

Please note that many of the hazard models developed outside of GEM may use different methods than those described here. However, the following is a description of the practices that we at GEM use for the development of our models.

8 Fault geometry and mapping

Fault geometry in map view is constrained through geologic mapping, while the geometry in cross-section view is estimated from geologic cross-section construction or based on the fault kinematics and local focal mechanisms.

In seismic hazard work, almost all faults are given as the geographic coordinates of the fault trace, with an average dip that is used to build a three dimensional representation of the fault surface.

Mapping faults for hazard work is a complicated endeavor; a more in-depth description of this process can be found at the GEM Hazard Blog.

9 Assessing fault activity

Fault activity is assessed through a variety of criteria. The first are instrumental, historical or paleoseismological evidence for earthquakes along the fault; second is strain accumulation that is rapid and localized enough to be measurable through geodetic techniques (GPS, InSAR, optical geodesy); and third is Quaternary geomorphic evidence such as fault scarps, offset streams, and so forth. If the evidence is strong in favor of activity, or a fault is thought to pose a great societal risk, then the fault will be included in the fault source model (with its appropriate uncertainty). If a fault does not display convincing evidence for activity given these criteria, it will be omitted from the fault source model.

9.1 Kinematics

The kinematics of faults, if they are not previously known from earlier studies, are inferred from the topographic and geomorphic expression of the fault, from local focal mechanisms, and from regional geodetic strain information. It is not typical that much confusion or ambiguity exists between normal, strike-slip and reverse faults, since these all have very distinct geomorphic expressions; the more confusing cases tend to be when oblique slip may be present, or when fault kinematics have changed over the millions of years of fault activity, and the topography from the previous tectonic regime is still present. It is more challenging to distinguish between left-slip and right-slip strike-slip faults if no focal mechanisms

or GPS data are available, but it is still generally possible (particularly by looking at bends or stepovers in the fault and the kinematics of faults in these regions).

9.2 Slip Rates

Fault slip rates are generally assessed through formal geologic studies of individual faults through neotectonic and paleoseismic studies, or from geodetic studies of faults or fault networks.

These are complicated and time-intensive investigations, and we at GEM do not generally do this work. Instead, we gather and evaluate the existing literature on faults in a region. There are always many more faults in an area than those that have had formal study, so we will use the rates given in the literature for the faults that have information, and then generalize that information in the context of geodetic strain rate data to infer what the slip rates may be for other structures. For example, faults or fault segments that lie along strike of faults with known slip rates are likely to have similar rates. The regional geodetic strain field provides an overall budget for slip rates within the region: if an area has 6 mm/yr of dextral shear, and the major fault in the area has a known slip rate of 3 mm/yr, then the other faults in the area cannot have dextral slip rates that add up to more than 3 mm/yr. The summed slip rate on faults may be less than the overall geodetic strain, though: some amount of strain may not be distributed on smaller structures or through continuous, plastic deformation of the crust instead of being localized on the major faults in a dataset.

9.3 Seismogenic thickness

The seismogenic thickness of a fault is the total vertical distance between the upper and lower edges of the fault that rupture in a full-length earthquake. It is thought to be a consequence of the frictional stability of the fault materials (and the encompassing crust) at the varying temperature, pressure and fluid contents through the crust. The upper limit of fault slip, the upper seismogenic depth, is usually considered to be the surface of the earth though in some instances (such as subduction zone interfaces) it may be lower. The lower limit is variable based on tectonic environment and the frictional characteristics of the fault materials.

To paint in broad brush strokes, within the continents, normal faults occupy hotter areas of the crust and rupture from (near) the surface to 10-15 km depth; the crust in reverse faulting environments is often colder and the faults will rupture from 15-25 km depth to the surface. Strike-slip faults occupy all environments, so rupture can be from the surface to 10-25 km depth.

Oceanic faults have more variability. Subduction zone interfaces can rupture to near 50 km depth, as they are very cold. Intraplate strike-slip faults can also rupture to >30 km depth, which is well into the mantle in oceanic lithosphere. Hill et al. (2015) report that the 2012 Wharton Basin earthquake east of Indonesia may have ruptured to 50 km. Oceanic spreading ridges and associated transform faults are very hot. Normal faulting does not

produce large earthquakes and the lower depth is probably ~5 km. Associated transforms are slightly cooler and faulting will extend a bit deeper.

The most sound way to assess this is to look at finite fault inversions for the largest earthquakes in a region, if these exist. Lacking this, geodetic techniques may sometimes reveal a value indicating the lower limit of fault locking, although the uncertainties are usually quite large (and underestimated). Similarly, small to microseismicity in a region can give some constraints, but be aware that small earthquakes can occur at much deeper levels in the crust than large ones, because those earthquakes can occur in unfaulted rock that exhibits stick-slip frictional behavior and brittle failure to a greater depth than mature faults with well-developed fault gouge zones and circulating fluids.

10 Building Fault Source Models

Fault source models are usually created by creating three-dimensional fault surfaces and providing information about the style, magnitudes and frequencies of earthquakes that may occur on the fault surface.

10.1 Geometry

Fault geometries are generally created as extrusions of the fault trace (or simplified trace) at a constant dip down to some limit, usually the lower boundary of the seismogenic thickness. Within OpenQuake, these are referred to as 'simple faults'.

In some instances, the geometry of a fault may change sufficiently down-dip that a more complicated representation is warranted. These are known as 'complex faults' in OpenQuake; they are represented by sets of lines of equal depth. OpenQuake then interpolates between these lines to make the fault surface. At GEM, we primarily use complex faults for subduction interfaces.

10.2 Magnitude-Frequency Distributions

The occurrence of earthquakes on a fault is parameterized through magnitude-frequency distributions (MFDs). These give the magnitudes of all the earthquakes on a fault that are to be modeled, and the frequency (or annual probability of occurrence) of earthquakes of the corresponding magnitudes.

The two most common types of MFDs are truncated Gutenberg-Richter distributions, and characteristic distributions. Other MFDs exist that may be hybrids or based on other statistical models, but these are less commonly implemented in seismic hazard analysis. At GEM, we typically use the truncated Gutenberg-Richter distribution, but many other institutions use characteristic fault sources as well. It is still scientifically unknown what the 'true' distribution is and to what degree this changes for different faults, so the choice may come down to pragmatism, familiarity, preference and tradition.

Truncated Gutenberg-Richter distributions are typical Gutenberg-Richter Distributions that are bounded (truncated) by minimum and maximum magnitudes for earthquakes, *M*min and *M*max. Within those bounds, they are parameterized by the *a* and *b* values.

*M*min and *M*max have to be chosen by the fault modeler. *M*min is usually chosen as the smallest earthquake worth modeling in a given model–lowering this value increases the computation time of the model but may not increase the accuracy of the hazard calculations; lower values are more common in smaller-scale studies. *M*max is not so easily determined. The common practice at GEM is to choose it based on the area of a fault surface and the use of an empirical magnitude-area scaling relationship such as that of Wells and Coppersmith (1984) or the more updated Leonard (2012). *M*max then represents a typical full-fault rupture. However, these scaling relationships are statistically-derived and a good amount of variation is present. If there is convincing evidence of larger *M*max on a given fault than the scaling relationship predicts, one should of course choose that larger value.

The *a* and *b* values also need to be determined for each fault. Common practice is to take the *b*-value for a broader tectonic region that encompasses the fault derived from the instrumental seismic catalog, and apply that *b*-value to every fault within the region. There are a few theoretical reasons why this should not be absolutely correct: primarily, the sum of multiple truncated Gutenberg-Richter distributions will not produce a Gutenberg-Richter distribution (in mathematical terminology, the truncated GR distribution is not Levy stable). However, it is exceedingly rare for any empirical constraints on *b*-values for individual faults to exist, so this is a pragmatic compromise.

The *a*-values are chosen so that the total moment release rate adds up to the seismic moment accumulation rate. To make this calculation, the total moment accumulation rate is calculated as the product of the fault area, the shear modulus of the rock encasing the fault, and the fault slip rate. Then, the 'aseismic coefficient', which is the fraction of this total moment accumulation rate that is not released through earthquakes, is subtracted (note that in the case of creeping faults, this moment may never physically be stored in the crust as elastic strain; nevertheless the calculation will be the same). Finally, the *a*-value is chosen so that the total amount of seismic moment released annually (on average) by all of the earthquakes on the fault equals the annual moment accumulation.

Characteristic distributions are narrow distributions that typically represent full-length rupture of a given fault. The *M*max values are chosen through fault scaling relationships or inferences from paleoseismic data. These ruptures may also occur quasi-periodically (as opposed to uniformly randomly) though this sort of time-dependence is not often used at GEM.

11 References

Hill, Emma M., et al. “The 2012 Mw 8.6 Wharton Basin sequence: A cascade of great earthquakes generated by near-orthogonal, young, oceanic mantle faults.” Journal of Geophysical Research: Solid Earth 120.5 (2015): 3723-3747. https://doi-org.www2.lib.ku.edu/10.1002/2014JB011703

Leonard, Mark. “Earthquake fault scaling: Self-consistent relating of rupture length, width, average displacement, and moment release.” Bulletin of the Seismological Society of America 102.6 (2012): 2797-2797. https://doi-org.www2.lib.ku.edu/10.1785/0120120249

Wells, Donald L., and Kevin J. Coppersmith. “New empirical relationships among magnitude, rupture length, rupture width, rupture area, and surface displacement.” Bulletin of the seismological Society of America 84.4 (1994): 974-1002.

12 Types of MFDs

In probabilistic seismic hazard analysis (PSHA), source models require a defined occurrence rate for earthquakes of each considered magnitude, e.g., a magnitude-frequency distribution (MFD). These rates are determined either by statistically analysing the observed seismicity over instrumental and historic time scales, or-for well characterized sources—by using the fault dimensions and slip rates to model recurrence.

Regional models built by GEM use the following common approaches to characterize seismicity rates.

12.1 Gutenberg-Richter

The Gutenberg-Richter MFD allows earthquake sources to generate earthquakes of different magnitudes. *Gutenberg and Richter (1944)* were the first to develop a functional form for the relationship between earthquake magnitude and occurrence rate, resolving a negative exponential distribution:

$$logN = a - bm \tag{1}$$

(2)

where *N* is the annual rate of earthquakes with $M > m$, *a* is the rate of all earthquakes, and *b* is the relative distribution of earthquakes among magnitudes. A higher *b*-value indicates a larger proportion of seismic moment released by small earthquakes. *a* and *b* are resolved from the available observations. Usually, *b* is close to 1.0.

12.1.1 Truncated Gutenberg-Richter

A traditional Gutenberg-Richter MFD allows for earthquakes of any magnitude, but in reality, the source in question may not be capable of producing earthquakes beyond a certain threshold. For example, fault dimensions physically limit earthquake magnitude, or the observed earthquake magnitudes saturate. To account for these constraints, a truncated MFD is used to specify a maximum magnitude (*Mmax*), simply by cutting the MFD at this magnitude. The MFD is additionally cut at a minimum magnitude ("double-truncated"), below which earthquakes are not contributing to the hazard in ways significant to engineering.

Truncated Gutenberg-Richter MFDs are commonly used in hazard models build by the GEM Secretariat. Where MFDs are produced for a source zone, such as for distributed or inslab seismicity, the upper magnitude is usually determined by adding a delta value (e.g., *MW*0.5) to *Mmax* in the earthquake catalogue or subcatalogue used to produce the MFD. This is

based on the premise that the observation period is too short to have experienced a true *Mmax* earthquake.

GEM models typically use the methodology of Weichert (1985) to compute double-truncated Gutenberg-Richter MFDs for seismic source zones, which allows for the use of different observation periods for different earthquake magnitudes (e.g., a completeness threshold).

If a seismicity distribution is not explicitly available, an MFD of this form can also be computed from a seismic moment budget using strain rates, fault dimensions, and assumed magnitude ranges and *b*-values. For models built internally by GEM, we apply this to faults with available slip rates. This methodology is described in Section 7.5.

12.2 Characteristic

Some sources do not produce earthquakes that follow the Gutenberg-Richter distribution, but instead tend to host earthquakes of nearly the same magnitude, e.g., a characteristic earthquake. In this case, an earthquake with a moderate to high magnitude occurs more frequently than would be suggested by a Gutenberg-Richter MFD. For sources of this type, the MFD reveals more frequent occurrences concentrated around the most-likely/characteristic magnitude earthquake, for example using a boxcar or Gaussian distribution (e.g., *Youngs and Coppersmith, 1985*, or *Lomnitz-Adler and Lomnitz, 1979*).

Though the *Youngs and Coppersmith* (*1985*) MFD is technically a hybrid MFD, incorporating both a characteristic component and a Gutenberg-Richter component at lower magnitudes, it is typically often categorized as a characteristic MFD. GEM uses this MFD in a few models built in-house, such as the Philippines (Section **??**) model, where sensitivity testing indicated that it produced a better fit to the regional seismicity than a double-truncated GR for crustal faults.

12.3 Hybrid types

Some subduction interface source models built by the GEM secretariat use a hybrid approach that combines the Gutenberg-Richter MFD with a characteristic MFD. The latter approach derives a double truncated Gaussian distribution to model occurrence of the maximum magnitude (*M*max) earthquake that an interface segment can theoretically support (herein called the "characteristic earthquake").

The magnitude and occurrence rate of the characteristic earthquake for an interface segment are based on the fault area (e.g., from the complex fault output by the Subduction Toolkit, see Section 17.1), the convergence rate, and a seismic coupling coefficient. We choose between three recent scaling relationships for subduction interfaces that compute magnitude from fault area: *Strasser et al.* (*2010*), *Allen and Hayes* (*2017*), and *Thingbaijam and Mai* (*2017*). We use published convergence rates and seismic coupling coefficients to determine the time needed to accumulate enough strain for the characteristic earthquake.

The coupling parameter is often challenging, in large part due to the scarcity of land and thus GPS measurements in close proximity to subduction zones. Where no other model is available, we take values from *Heuret et al.* (*2011*) or *Scholz and Campos* (*2012*), but cautiously, as many sometimes these values are suspiciously low (e.g., <0.1 where instrumentally recorded earthquakes *M*>8.0 have occurred.)

The characteristic MFD is combined with the Gutenberg-Richter MFD into a hybrid MFD by finding the intersection point of the two MFDs, and taking the Gutenberg-Richter occurrence rate below the intersection magnitude, and the characteristic rate above that magnitude.

12.4 References

Allen, T. I., & Hayes, G. P. (2017). Alternative rupture-scaling relationships for subduction interface and other offshore environments. *Bulletin of the Seismological Society of America*, 107(3), 1240-1253.

Gutenberg, B., & Richter, C. F. (1944). Frequency of earthquakes in California. *Bulletin of the Seismological Society of America*, 34(4), 185-188.

Heuret, A., Lallemand, S., Funiciello, F., Piromallo, C., & Faccenna, C. (2011). Physical characteristics of subduction interface type seismogenic zones revisited. *Geochemistry, Geophysics, Geosystems*, 12(1).

Lomnitz-Adler, J., & Lomnitz, C. (1979). A modified form of the Gutenberg-Richter magnitude-frequency relation. *Bulletin of the Seismological Society of America*, 69(4), 1209-1214.

Scholz, C. H., & Campos, J. (2012). The seismic coupling of subduction zones revisited. Journal of Geophysical Research: *Solid Earth*, 117(B5).

Thingbaijam, K. K. S., Martin Mai, P., & Goda, K. (2017). New empirical earthquake source-scaling laws. *Bulletin of the Seismological Society of America*, 107(5), 2225-2246.

Strasser, F. O., Arango, M. C., & Bommer, J. J. (2010). Scaling of the source dimensions of interface and intraslab subduction-zone earthquakes with moment magnitude. *Seismological Research Letters*, 81(6), 941-950.

12.5 Characterizating and processing seismic catalogues

Much of PSHA depends on the assumption that future seismicity will occur near observed past seismicity, and at rates that can be approximated by empirical or physical models. Thus, the early steps in PSHA include compiling and processing an earthquake catalogue. Beyond collecting instrumental and historic earthquake records, catalogues must be homogenized (expressed in uniform units), declustered (devoid of aftershocks and foreshocks), and filtered for completeness. The assumptions and uncertainties in the catalogue should be well understood by the modeler.

Most source types used in hazard models built by the GEM Secretariat use magnitude-frequency distributions (MFDs, Section 11.1) based on seismicity. Together with ground motion prediction equations (GMPEs), MFDs govern the computed hazard levels for time frames of interest, and so their robust calculation - and thus careful preparation of the input catalogue - is critical.

Here, we describe the ISC-GEM extended catalogue (*Weatherill et al., 2016*), which contributes the majority of earthquakes used in hazard models built internally by GEM; the workflow for combining other earthquake records with the ISC-GEM catalogue; and the remaining steps to prepare the catalogue for rate and spatial analysis. We emphasize that while most of these steps are routinely applied outside of GEM models, the following explanations only account for our own best practices.

13 The ISC-GEM catalogue

The ISC-GEM catalogue is a compilation of earthquake bulletins for seismicity occurring in the range 1900-2015. This catalogue sources records from numerous agencies to include the record deemed most accurate for each event, ensuring that no duplicates are included, and magnitudes are homogenized to *MW*. The most recent catalogue updates were completed by *Weatherill et al. (2016)* using the GEM Catalogue Toolkit, totaling 562 840 earthquakes with *MW* 2.0 to 9.6, and producing what is herein called the ISC-GEM extended catalogue. This current version is motivated by initiatives to improve regional and global scale seismicity analyses, hazard and otherwise.

Regional models developed by the GEM Secretariat use the ISC-GEM extended catalogue, augmented by data from local agencies when possible.

14 GEM Historical Earthquake Catalogue

The GEM Historical Earthquake Catalogue (*Albini et al., 2013*), includes large earthquakes (*M*>7) from before the instrumental period (1000-1903) that have been carefully reviewed to estimate a location and magnitude. The completeness of this catalogue is highly variable across the globe, and depends on how long each location has been inhabited, and the availability and quality of documentation on earthquakes occurring in this period.

15 Processing of seismicity catalogues

15.1 Catalogue homogenization

In order to use the bulletins from multiple agencies together in statistical analyses, records must be homogenized to meet the same criteria, e.g., to use the same measure of magnitude. Usually, moment magnitude (*MW*) is selected, since it does not saturate at high magnitudes. Thus, magnitudes reported in other scales must be converted. When possible, this is done using empirical relations developed for independent local datasets, but relies on global relations when too few calibration events are available.

The homogenization methodology used to build the ISC-GEM extended catalogue is described in detail in *Weatherill et al. (2016)*.

15.2 Completeness analysis

Catalogue completeness analysis accounts for the variability in instrumentation coverage throughout the catalogue duration, admitting that any catalogue is missing earthquakes beneath a magnitude threshold. This type of filtering prevents rate analysis of an incomplete catalogue - a modeling mistake that will propagate into hazard estimates. Importantly, completeness analysis must be applied to a declustered catalogue as to not confuse dependent earthquakes (such as aftershocks) with magnitude completeness.

The completeness algorithms that are applicable to *any* instrumental catalogue must depend on properties of the earthquakes, and not the stations, thus focusing on the statistics of the catalogue sample rather than the probability that a station at a known position would record an earthquake. The most common algorithmic method is by Stepp (1971), which compares the observed rate of seismicity to a predicted Poissonian rate for each magnitude, and returns a spatially constant table of time-variable magnitude thresholds. Importantly, the validity of this methodology is subject to the judgement of the user.

The Stepp (1971) is implemented in the OpenQuake Engine, and used in some steps of the modeling procedure for hazard models built by the GEM Secretariat. In other cases, we determine the completeness manually from 3D histograms that count earthquakes for magnitude-time bins, visually identifying the timings at which the occurrences rates stabilize.

15.3 Declustering

Catalogue declustering is applied in order to isolate mainshock earthquakes - that is, earthquakes that occur independently of each other - from a complete catalogue. The resulting declustered catalogue should therefore reflect the Poissonian rate at which earthquakes occur within a greater tectonic region. PSHA aims to model the hazard from sesimicity occurring at this background Poissonian rate.

Declustering algorithms identify mainshocks by comparing individual earthquakes to the "cluster" of earthquakes that occurred within a given proximity and time to that earthquake, choosing the largest for a given set of magnitude-dependent "triggering windows". The theory of declustering algorithms is described in detail in *Stiphout et. al., 2012*. The OpenQuake Hazard Modeler's Toolkit provides three different windowing options: the original implementation of Gardner and Knopoff (1974), and additionally the configurations of Uhrhammer (1986) and Gruenthal (see Stiphout et al., 2012).

In subduction zones or other complex environments, we first classify the seismicity by tectonic domain (described below), and then decluster groups of domains within which we expect seismicity to interact (i.e., interface mainshocks can trigger crustal aftershocks), and then separate the deemed mainshocks into subcatalogues based on their tectonic classification. We typically use two groups: crustal, interface, and shallow slab seismicity (that beneath the interface but with intraslab mechanisms); and deep intraslab seismicity. The declustering algorithm comparing epicentral (*not* hypocentral) proximities, and thus, declustering by groups is crucial for seismicity within slab-type volumes.

16 Classification of seismicity

The workflow used by GEM to construct seismic source models in complex tectonic regions is dependent on the use of classified seismicity, that is, the assignment of each earthquake to a tectonic domain. Separating earthquakes in this manner allows us to compute MFDs from only the seismicity occurring within a delineated domain, thus more accurately characterizing individual seismic sources or source zones. For example, in subduction zones, we separate earthquakes occurring on the interface itself from those within the downgoing slab or the overriding plate. This allows us to model the hazard from these source types using the appropriate GMPEs.

At GEM, we classify seismicity using an procedure with similar theory to *Zhao et al., (2015)* and *Garcia et al., (2012)*, which assigns earthquakes to tectonic domains defined by the modeler. In subduction zones, earthquakes are usually categorized as crustal, interface, or intraslab based on hypocentral proximity to the Moho, and the interface and slab-top complex surfaces defined by the Subduction Toolkit (Section 17.1). Where subduction zones are modeled as segmented interfaces or slabs, the domains are divided accordingly. Each tectonic domain is defined by a surface and a buffer region based on general characteristics of the corresponding cross sections. The modeler provides a tectonic hierarchy that chooses among multiple assignments for earthquakes occurring within overlapping buffers of two or more domains. Usually, we specify interface superseding intraslab, and intraslab superseding crustal. Earthquakes that do not correspond to any of the defined domains are deemed "unclassified".

The classification routine includes workarounds to correct some common misclassifications, such as to seclude dominant groups of earthquakes beneath a polygon (e.g., volcanic events); to classify large magnitude earthquakes from historic catalogues only by epicenter;

and the ability to manually classify earthquakes by their event IDs.

17 References

Albini P., Musson R.M.W., Rovida A., Locati M., Gomez Capera A.A., and Viganò D. (2014). The Global Earthquake History. Earthquake Spectra, May 2014, Vol.30, No.2, pp. 607-624. http://doi.org/10.1193/122013EQS297

Gardner, J. K., and Leon Knopoff. "Is the sequence of earthquakes in Southern California, with aftershocks removed, Poissonian?." Bulletin of the Seismological Society of America64.5 (1974): 1363-1367.

Stepp, J. C. (1971). "An investigation of earthquake risk in the Puget Sound area by the use of the type I distribution of largest extreme". PhD thesis. Pennsylvania State University (cited on pages 9, 25–27).

Stiphout, T. van, J. Zhuang, and D. Marsan (2012). Theme V -Models and Techniques for Analysing Seismicity. Technical report. Community Online Resource for Statistical Seismicity Analysis. URL: http://www.corssa.org.

Uhrhammer, Robert A. "SEISMICITY RECORD, M> 2.5, FOR THE CENTRAL." Clement F. Shearer (1985): 199.

Weatherill, G. A., M. Pagani, and J. Garcia. "Exploring earthquake databases for the creation of magnitude-homogeneous catalogues: tools for application on a regional and global scale." Geophysical Journal International 206.3 (2016): 1652-1676.

17.1 Characterizing and modelling subduction sources

Subduction zones are plate margins where one tectonic plate 'subducts' or is thrust beneath another plate. These zones produce most of the seismicity on Earth. The zones can be complex, producing earthquakes at the interface or 'megathrust' fault between the plates, in the downgoing plate or 'slab', and in the deforming region at the margin of the upper, overriding plate. For hazard models produced by the GEM Secretariat, the plate interface and the subducting slab are characterized and modeled with subduction-specific tools we have developed alongside our modeling efforts, while the deformation within the upper plate is modeled as part of the active shallow crust.

18 Subduction interface

Among PSHA models, various source model approaches are used to model interface seismicity. Models produced by GEM use OpenQuake complex faults (surfaces with complex geometry) to account for subduction interface seismicity, and float all possible ruptures within specified magnitude limits and have a given rupture aspect ratio across the meshed surface. In some cases, we segment the surfaces along-strike to define firm barriers to rupture or capture changes in subduction characteristics. We use two predominant approaches to compute magnitude-frequency distributions (MFDs) and maximum magnitudes of the interface segments. Both use recorded instrumental (and sometimes historical) seismicity that can be attributed to the respective interface segment (classified using the methodolgy described in Section 16), fitting a Gutenberg-Richter (a negative exponential) distribution to the seismicity. One approach also includes a characteristic component, computed from the area of the interface surface, the local convergence rate, and the degree of seismic locking (a seismic coupling coefficient). MFD construction is explained in detail in Section 11.1.

19 Slab

Hazard models built by the GEM Secretariat account for intraslab seismicity using non-parametric ruptures (sources with predefined geometry) that fit within a slab volume of uniform thickness. The ruptures correspond to virtual faults within a meshed approximation of the slab volume, and forces ruptures to fit within the slab. Like the interface, the slab volume can be segmented, however here, boundaries only seldom indicate barrier to rupture (such as at a slab tear) and are more commonly used to reflect change in seismicity rate. For each slab segment, we compute a single Gutenberg-Richter MFD from the slab segment subcatalogues produced during tectonic classification (Section 16), assuming constant rates throughout each segment. Currently, moment rates are distributed uniformly among the computed ruptures, but future development will include a smoothing component.

20 The Subduction Toolkit: building the geometry of the interface surface and slab volume

Alongside the PSHA models that incorporate subduction zones, GEM has developed the Subduction Toolkit, which uses an interactive workflow to build the subdction interface and slab top geometry, an integral step in producing the subduction source model.

The subduction geometries are based on trench axes from the GEM Active Faults Database along with several geophysical datasets and models. The toolkit projects swaths of geophysical data onto cross sections along a trench axis, which are used to guide depth picking for the interface and slab upper surface. These depth profiles are then stitched together to form OpenQuake complex fault surfaces, which are used as reference frames for catalogue tectonic classification (Section 16), and for defining subduction source geometry (described above).

The data plotted on the cross sections is meant to illuminate the subsurface subduction structures and tectonic processes that contribute to seismic hazard (e.g., Figure 13). The most commonly used data include:

- hypocenters from ISC-GEM catalogue (*Weatherill et al., 2016*)
- centroid moment tensors (CMTs) from the Global CMT project (*Dziewonski et al., 1981*; *Ekstrom et al., 2012*)
- Moho depth estimates from Lithos1.0 (*Pasyanos et al., 2014*) and Crust1.0 (*Laske et al., 2013*)
- Slab depth estimates from Slab1.0 (*Hayes et al., 2011*) and Slab2.0 (*Hayes et al., 2018*)
- Shuttle Radar Topography Mission (SRTM) topography (*Farr, 2007*)
- General Bathymetric Charts of the Ocean (GEBCO) bathymetry (*Weatherall et al., 2015*)
- Volcano locations

Initially, the cross sections are automatically generated at a specified increment along the trench axis that balances data density with resolution, with azimuths perpendicular the trench. The cross section origins and azimuths can then be adjusted manually, and additional cross sections added where necessary.

The final depth profiles (or a subset) are stitched together to form an OpenQuake complex fault surface. The Toolkit allows for the full extent of the profiles to be considered in subsequent steps, or a depth range can be defined. We use these capability to separate the subduction interface from the deeper slab, and to segment the surfaces along strike (see above).

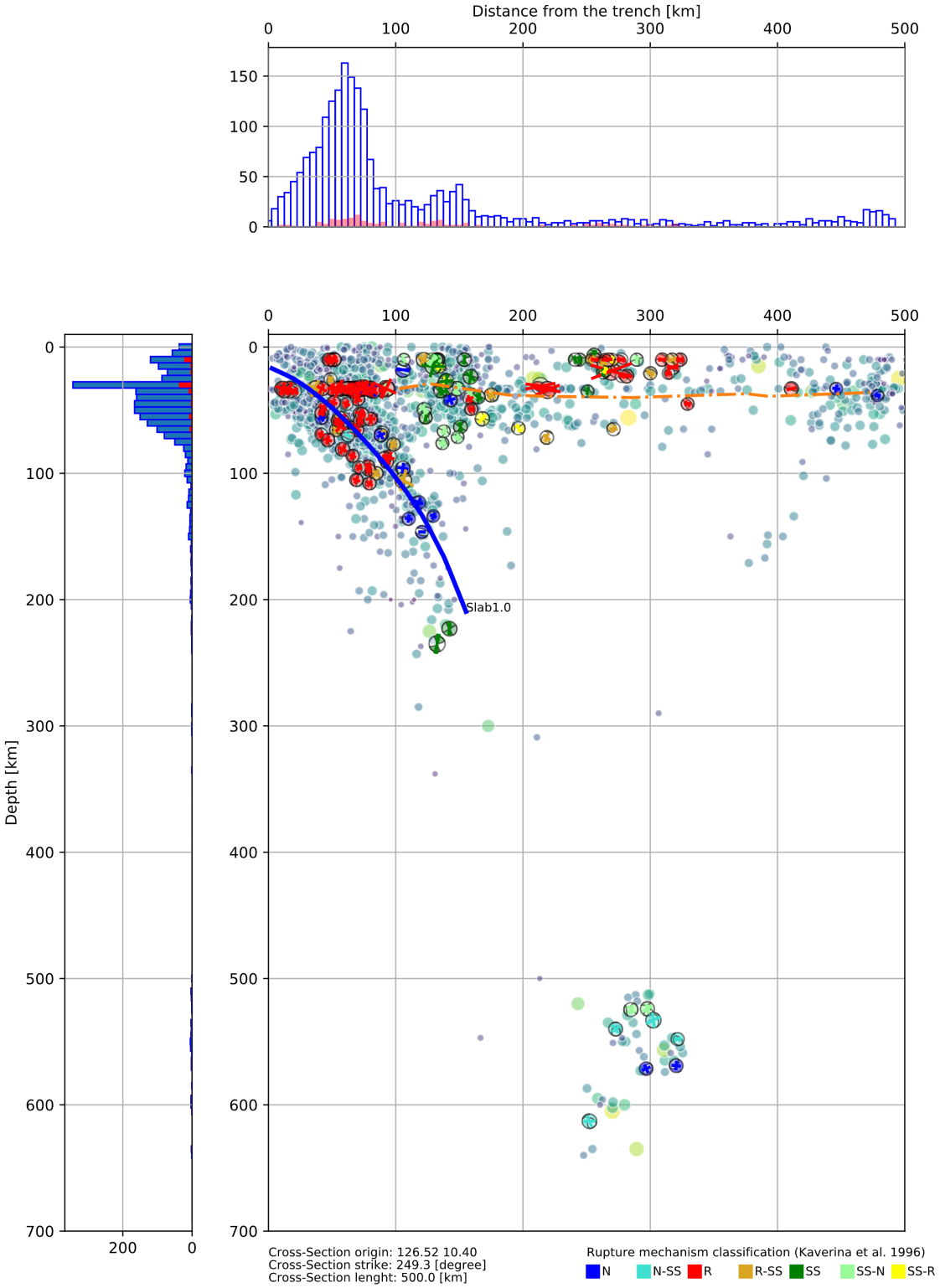

Figure 13 *– Example cross-section of a subduction zone from the Philippines*

21 References

Dziewonski, A. M., T.-A. Chou and J. H. Woodhouse, Determination of earthquake source parameters from waveform data for studies of global and regional seismicity, J. Geophys. Res., 86, 2825-2852, 1981. doi:10.1029/JB086iB04p02825

Ekström, G., M. Nettles, and A. M. Dziewonski, The global CMT project 2004-2010: Centroid-moment tensors for 13,017 earthquakes, Phys. Earth Planet. Inter., 200-201, 1-9, 2012. doi:10.1016/j.pepi.2012.04.002

Farr, T.G., Rosen, P.A., Caro, E., Crippen, R., Duren, R., Hensley, S., Kobrick, M., Paller, M., Rodriguez, E., Roth, L. and Seal, D., 2007. The shuttle radar topography mission. Reviews of geophysics, 45(2), doi:10.1029/2005RG000183.

Hayes, Gavin P., David J. Wald, and Rebecca L. Johnson. "Slab1. 0: A three-dimensional model of global subduction zone geometries." Journal of Geophysical Research: Solid Earth 117.B1 (2012).

Hayes, G. P., Moore, G. L., Portner, D. E., Hearne, M., Flamme, H., Furtney, M., & Smoczyk, G. M. (2018). Slab2, a comprehensive subduction zone geometry model. Science, 362(6410), 58-61.

Laske, Gabi, et al. "Update on CRUST1. 0—A 1-degree global model of Earth's crust." Geophys. Res. Abstr. Vol. 15. Vienna, Austria: EGU General Assembly, 2013.

Pasyanos, Michael E., et al. "LITHO1. 0: An updated crust and lithospheric model of the Earth." Journal of Geophysical Research: Solid Earth 119.3 (2014): 2153-2173.

Weatherall, P., K. M. Marks, M. Jakobsson, T. Schmitt, S. Tani, J. E. Arndt, M. Rovere, D. Chayes, V. Ferrini, and R. Wigley (2015), A new digital bathymetric model of the world's oceans, Earth and Space Science, 2, 331–345, doi:10.1002/2015EA000107.

Weatherill, G. A., M. Pagani, and J. Garcia. "Exploring earthquake databases for the creation of magnitude-homogeneous catalogues: tools for application on a regional and global scale." Geophysical Journal International 206.3 (2016): 1652-1676.

Last processed: Thursday 8th June, 2023 @ 18:13

www.globalquakemodel.org
If you have any questions please contact the GEM Foundation Hazard Team at: hazard@globalquakemodel.org